In Mabil Village, northern Catanduanes, there are several exposures of hydrothermal clay along the road which make it difficult to pass in the rainy weather. In this hydrothermal alteration zone, chalcedony films and impregnation of pyrite are observed in some places. The results of the assay are shown in Table 24. However, the alteration seems weak and the area seems barren.

Table 24 **Assay Results of the Mabil Mineral Occurrence**

	Au(g/t)	Ag(g/t)	Cu(%)	Fe(%)	Mo(%)	Pb(%)	Zn(%)	S(%)
CCR-022	nil	2	0.005	5.04	0.006	nil	0.007	0.572

2-5 Geochemical Survey (Stream Sediments)

2-5-1 Sampling

Sampling has been done along main rivers and their tributaries at sampling points selected beforehand to cover the whole island. The spacing of sampling points is 500m as a rule. Stream sediments have been taken at the center of the stream and sieved to -80 mesh fraction. Total number of stream sediment samples is 717. The localities of the samples are shown in PL-1 together with the localities of rock samples.

Samples have been dried in the air and devided into two portions, one for the Philippine side and the other for Japanese side. Then Japanese portions have been provided for chemical analysis.

2-5-2 Pathfinder Elements

Au, Ag, Cu, and related elements to the mineralization, i.e., As, Fe, Hg, Mo, Pb, S, Sb and Zn have been selected for chemical analysis.

Neutron activation analysis has been applied for analysis of Au. Induction furnace method has been applied for analysis of S. For other nine elements ICP-AES method has been applied.

The lower detection limit for the elements are as follows:

Au:1ppb, Ag: 0.2ppm, As·Pb·Sb·Zn: 2ppm, Cu·Hg·Mo:1ppm, Fe·S:0.001%

2-5-3 Analysis of Geochemical Data

(1) Statistic Processing

It is well known that frequency distribution of grades of elements in geochemical samples, especially in minor elements, generally shows logarithmic normal distribution. Therefore, common logarithm of the grade figures has been used for the interpretation. For the

convergence of statistical processing, the half figures of the lower detection limits have been used for samples which show lower grades than the lower detection limits. For Fe, there are some samples whose Fe grades exceed the upper detection limit. For these samples, the figure 19% was applied for their Fe grade, which is the average of Fe grades above the upper detection limit on the condition that grades over the limit follows logarrithmic normal distribution.

The maximum, minimum and average values together with the standard deviation for each element are shown in Table 25. Fig.25 shows correlation between each elemant. Table 26 shows the correlation coefficients between each element.

Table 25 **Basic Statistic Values of Elements (Stream Sediments)**

Element	Unit	Max.	Min.	Average	AV.-log	Std.Dev.
Au	ppb	4510	<1	110.7664	0.6405	1.0072
Ag	ppm	1.4	<0.2	0.1550	-0.9028	0.2304
As	ppm	94	<2	6.5258	0.4824	0.5342
Cu	ppm	425	24	103.9833	1.9888	0.1590
Fe	%	>15	2.78	10.0810	1.0317	0.2405
Hg	ppm	18	<1	0.6018	-0.2675	0.1345
Mo	ppm	8	<1	0.6799	-0.2251	0.1804
Pb	ppm	28	<2	2.6876	0.2334	0.3621
S	%	1.25	<0.001	0.0221	-2.0765	0.5329
Sb	ppm	12	<2	1.6360	0.1378	0.2268
Zn	ppm	424	22	133.5732	2.0869	0.1820

Table 26 **Correlation Coefficients between the Elements (Stream Sediments)**

	Au	Ag	As	Cu	Fe	Hg	Mo	Pb	S	Sb	Zn
Au	1.000										
Ag	0.044	1.000									
As	-0.031	0.174	1.000								
Cu	-0.011	-0.150	0.313	1.000							
Fe	-0.028	0.011	-0.143	-0.070	1.000						
Hg	0.006	-0.076	0.048	0.043	0.092	1.000					
Mo	-0.089	-0.159	0.140	0.183	0.137	0.125	1.000				
Pb	-0.141	-0.204	0.193	0.258	0.107	0.120	0.198	1.000			
S	0.104	-0.098	0.018	-0.040	-0.052	-0.022	0.038	0.078	1.000		
Sb	-0.109	0.074	0.286	0.048	-0.030	-0.014	0.199	0.087	0.030	1.000	
Zn	-0.250	0.065	-0.060	0.017	0.694	0.017	-0.044	0.022	-0.084	-0.017	1.000

There is positive correlation between Fe and Zn. Other elements show no correlation.

(2) Classification of Geochemical Anomaly Values

Lepeltier(1969), Sinclair(1976), and Govett et al. (1983) proposed some methods to set thresholds, i.e. a way using natural turning points in frequency distribution curves, a way

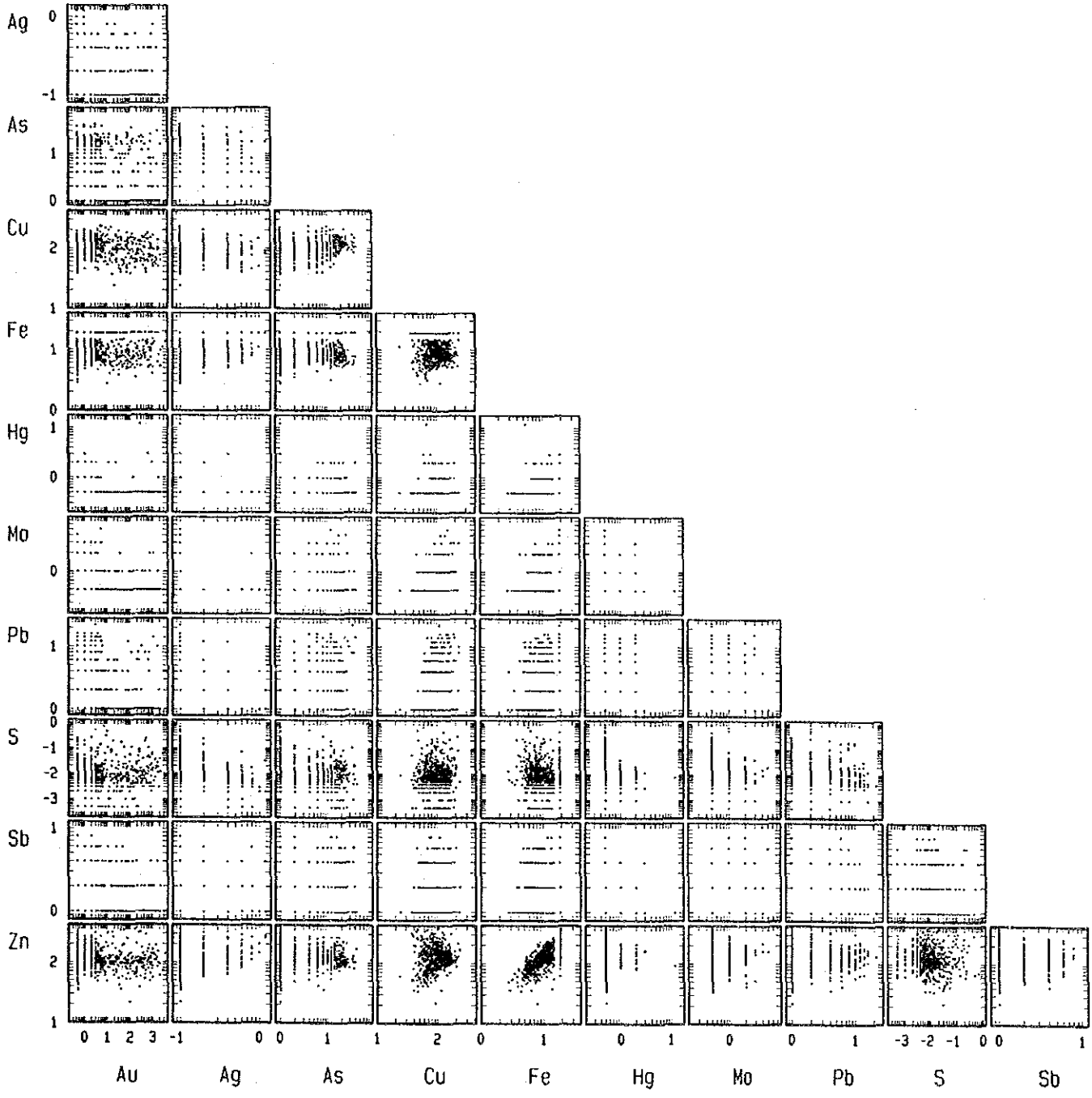

Fig.25 Scatter Diagram (stream sediments)

using turining points in cumulative frequency distribution curves, a way using average and standard deviation values,or a way based on percentiles, etc.

In this survey, average and standard deviation values together with frequency distribution and cumulative frequency distribution curves have been used to set thresholds. Fig.26 shows frequency distribution and cumulative frequency distribution of each elements. Table 27 shows the threshold values for each elements. For each element except for Fe, two steps of thresholds are set to distinguish especially high anomaly.

Table 27 **Classifications of Geochemical Anomalies (Stream Sediments)**

Au	M+σ(44.43ppb)	M+2σ(451.76ppb)
Ag	M+σ(0.21ppm)	M+2.5σ(0.47ppm)
As	M+σ(10.39ppm)	M+1.5σ(19.22ppm)
Cu	M+σ(140.56ppm)	M+2σ(202.70ppm)
Fe	M+σ(18.71%)	
Hg	M+σ(0.74ppm)	M+3σ(1.37ppm)
Mo	M+σ(0.90ppm)	M+2.5σ(1.68ppm)
Pb	M+σ(3.94ppm)	M+2σ(9.07ppm)
S	M+σ(0.03%)	M+2σ(0.10%)
Sb	M+σ(2.32ppm)	M+2.5σ(5.07ppm)
Zn	M+σ(185.74ppm)	M+2σ(282.43ppm)

2-5-4 Distribution of Geochemical Anomalies

Fig. 27 shows distribution of geochemical anmomalies of stream sediments.

(Au) Rather large anomaly zones for Au are distributed in the Dugui Too Area and the Carorongan Area. Small anomaly zones are disparsed around the Batalay Intrusives, in the Tilod, San Pedro, Libjo, Aroyao, and Solong Occurrences. In the mountainous area east of the Bato River, there are sporadic distribution of anomalies. Small anomaly zones are distributed in Gigmoto, Guiamlong and around Mabil.

The anomaly zone in Dugui Too is the largest and the most intense one of all. Many small intrusive bodies have been found to cause hydrothermal alteration in this area. Although quartz veins found in this area are rather small in scale, predominant quartz vein may be found by detailed geological survey.

The anomaly zone in the Carorongan Area is the second largest one. This anomaly zone spreads between the Manuria River and its tributary, the Carorongan River. Many quartz floats have been found in this area and quartz veins are considered to be exist in rather large area. Further geological survey is required to reveal the characteristics of the ore deposit.

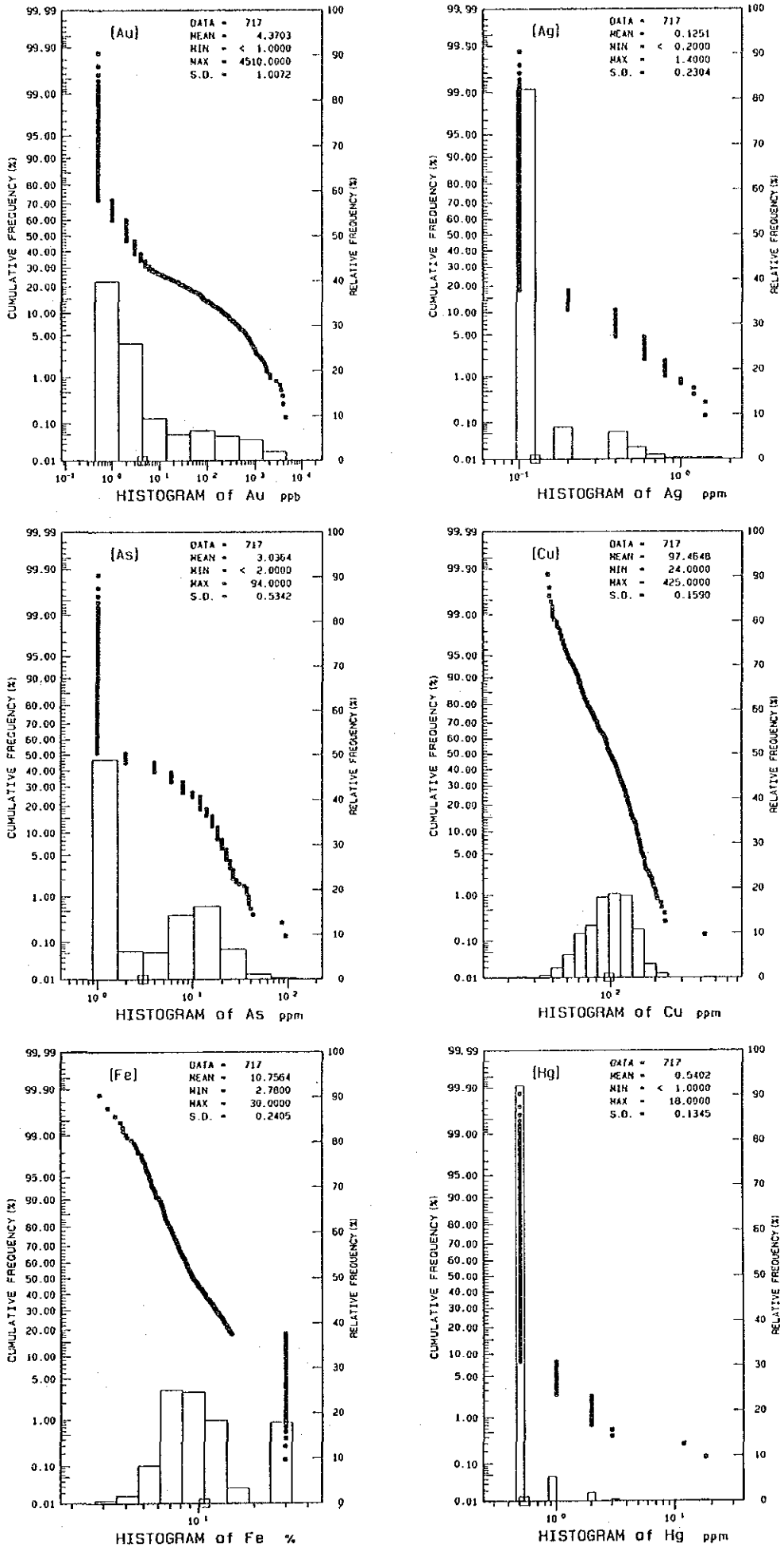

Fig.26 Frequency Distribution and Cumulative Frequency Distribution (stream sediments)(1)

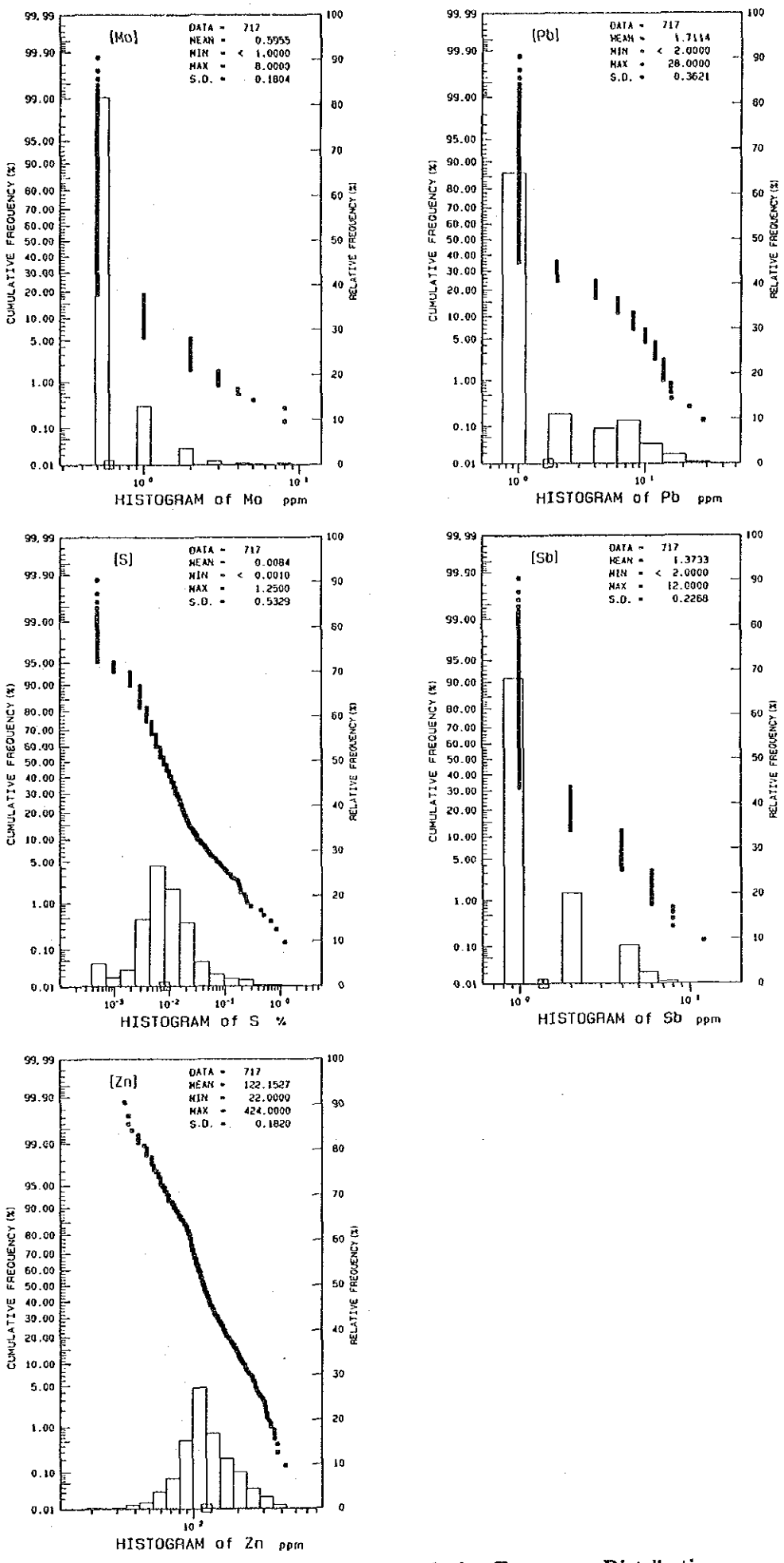

Fig.26 Frequency Distribution and Cumulative Frequency Distribution (stream sediments)(2)

(Ag) Fairly large Ag anomaly zones are distributed along the Manuria River, west of Carorongan Mineral Occurrence. Also around Soboc Village, which is located east of Carorongan Mineral Occurrence, there is a small and weak anomaly. In the Northern Block, small but rather intense anomalies are distributed in the lower reaches of the Inipan River and in the middle reaches of the Hilakan River. Also in the Northern Block, there are small and weak anomaly zones in the middle reaches of the Minaile River and the Talahib River, in the lower reaches of the Tabugoc River, along tributaries to the Pandan River and the Hilakan River, and around Mabini Village. Along the west coast, there are several small anomaly zones such as those along the Guiamlong River and in the upper reaches of the Hitoma River. Also in the middle reaches of the Maygnaway River a small anomaly zone is distributed. In the southern part of the island, there is an anomaly zone in the upper reaches of the Patorac River. There are small and weak anomaly zones in the Dugui Too Mineral Occurrence, east of the Solong Mineral Occurrence and in the area between Pagsagnahan and Kilikilihan.

(As) No correlation is observed between Au and As, and no anomaly zone is observed either in the Dugui Too Mineral Occurrence nor in the Carorongan Mineral Occurrence. There is a weak but large anomaly zone in the mountainous area east of the Bato River. Some strong anomalies are scattered in this area. Along a tributary to the Bato River, which joins the main stream at Pagsagnahan Village, there are some weak anomaly zones. A small but strong anomaly zone is distributed around the Tubli Mineral Occurrence, northwestern part of the island. Threre are many small and weak anomaly zones distributed in the area such as those in the upper reaches of the Mambang River and the Pandan River, along the Guiamlong River, in the upper and middle reaches of the Maygnaway River, around Bonagbonag Point, in the lower reaches of the Ananagnon River, north of Calolbon Town and in the area between Solong Mineral Occurrence and Aroyao Mineral Occurrence. Along the east coast there are also several small anomaly zones. Among these the one south of Gigmoto Town and the one around Tinaga Village are rather strong.

(Cu) A rather large anomaly zone is distributed in the area between Pagsagnahan and Kilikilihan. There are some anomaly zones along a tributary to the Bato River which joins the main stream at Pagsagnahan Village. The anomaly along the Kaglatawan River is especially strong. There is also a large anomaly zone along the Bato River between Pagsagnahan Village and Mabato Village.

(Fe) There are anomaly zones in the western and eastern area of the Northern Block, where basaltic rocks of the Yop Formation expose or underlie the Payo Formation. There is an

anomaly zone along the Kaglatawan River in the central part of the island. These anomalies are considered to be the halo of the rocks of the areas. On the other hand, in the Southern Block no conspicuous anomaly zone is observed in the area where the Yop Formation is distributed. This may mean the difference of characters between the Yop Formation of the North and Central Blocks and the Yop Formation of the Southern Block. There are sporadic anomalies in the Central Block where the Catanduanes Formation is widely distributed. Small anomaly zones are distributed in the area southwest of Pagsagnahan Village, around the Solong Mineral Occurrence, along the Balungbang River and around the Dugui Too Mineral Occurrence.

(Hg) A strong anomaly is distributed around Dugui Wala Village. There is a small anomaly zone in the middle reaches of the tributary of the Bato River, which joins the main stream at Pagsagnahan Village. A small and weak anomaly is observed in the middle reaches of the Panganiban River.

(Mo) A relatively large anomaly zone is distributed in the upper reaches of the tributary of the Bato River which joins the main stream at Pagsagnahan Village. There are small anomaly zones in the middle reaches of this river, in the upper reaches of the Bato River, in the mountainous area east of the Bato River, and around Mabato Village. There is relatively a large anomaly zone between Bato Town and Bagunbayan Village. There are also several small anomaly zones in the southern part and northern part of the island.

(Pb) There is a large anomaly zone along the tributary of the Bato River, which joins the main stream at Pagsagnahan Village. There is also a large but weak anomaly in the mountainous area east of the Bato River in which small strong anomaly zones are scattered. Around Tubli Village a small but strong anomaly zone is distributed.

(S) There is a large anomaly zone in the upper reaches of the Hilakan River. This anomaly is considered to be affected from the alteration zone in which silisified and pyritized zones have been observed in the geological survey of this area. A strong anomaly zone is also distributed in the lower reaches of the Malaquio River, northeast part of the island. In the area east of Bato Town there exist small anomaly zones. There are also anomaly zones around the Solong Mineral Occurrence and the Dugui Too Mineral Occurrence.

(Sb) A strong anomaly is distributed in the area between Mabil Village and the middle reaches of the Minaile River. Small anomalous zones are scattered in the island.

(Zn) Large and strong anomaly zones are consentrated in the Northern Block. There are small anomaly zones in the middle reaches of the Bato River and southwestern part of the island. Strong anomaly of Zn is restricted to the areas where the Yop Formation is distributed or their

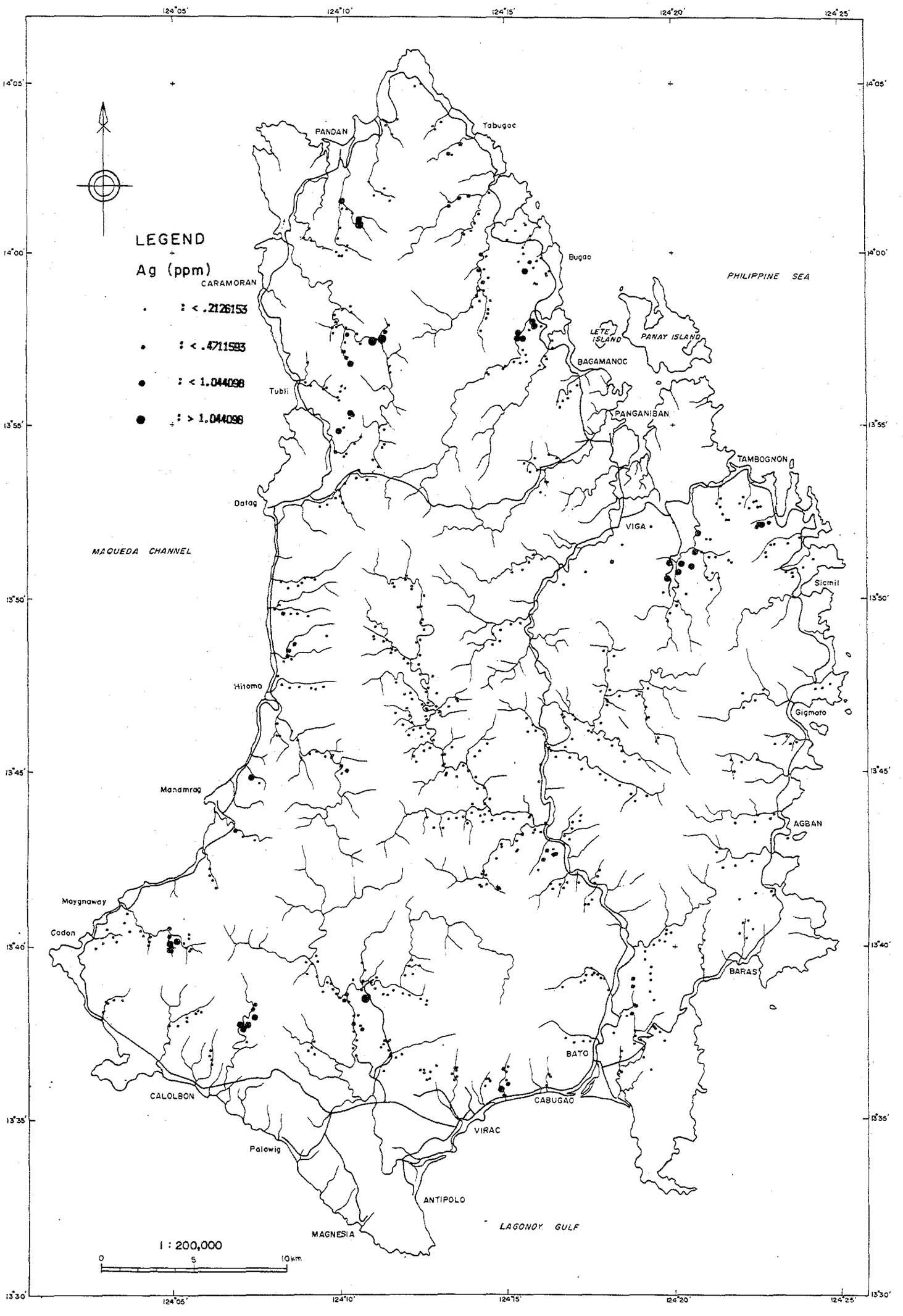

Fig.27 Geochemical Anomaly of Stream Sediments (1)

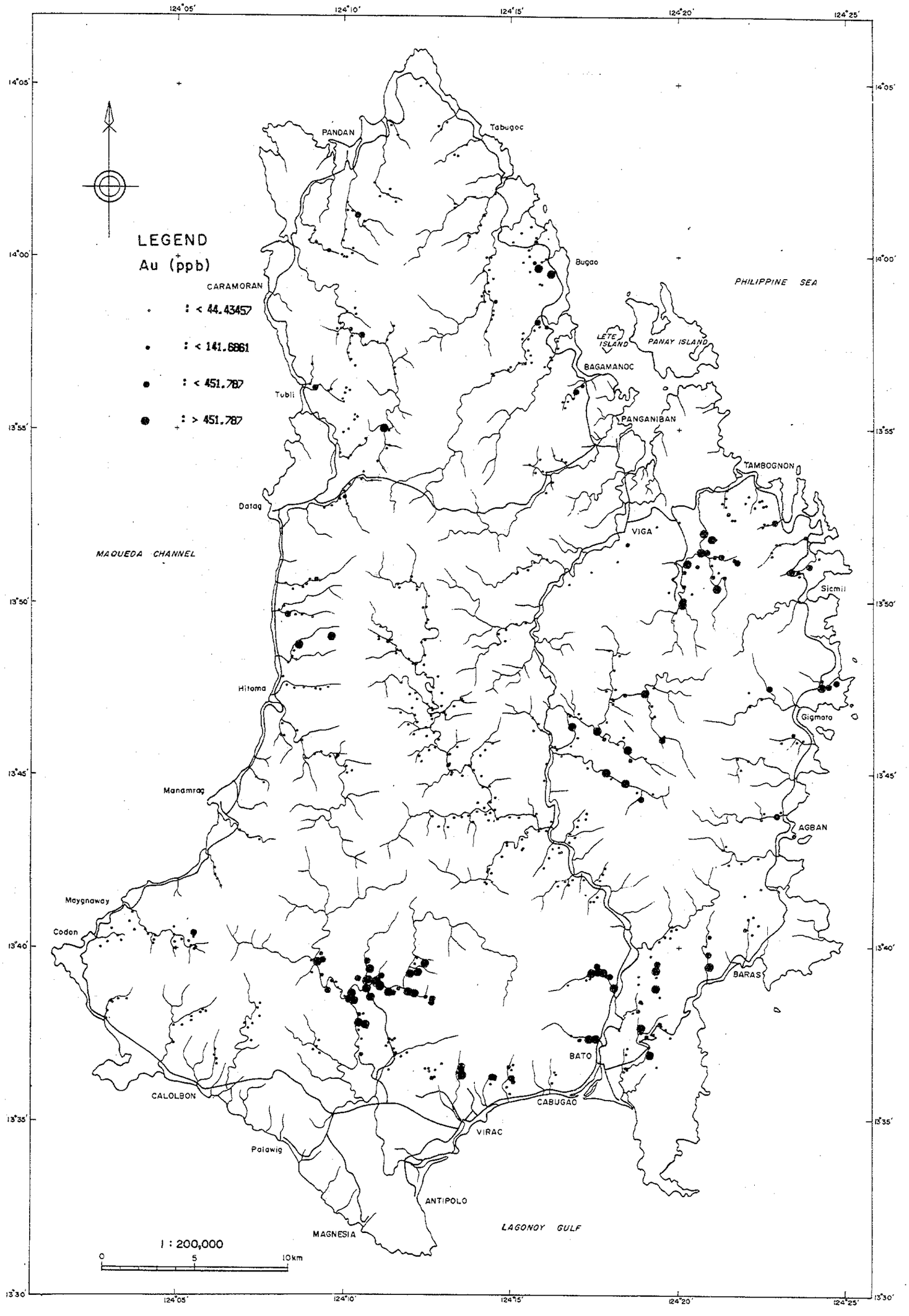

Fig.27 Geochemical Anomaly of Stream Sediments (2)

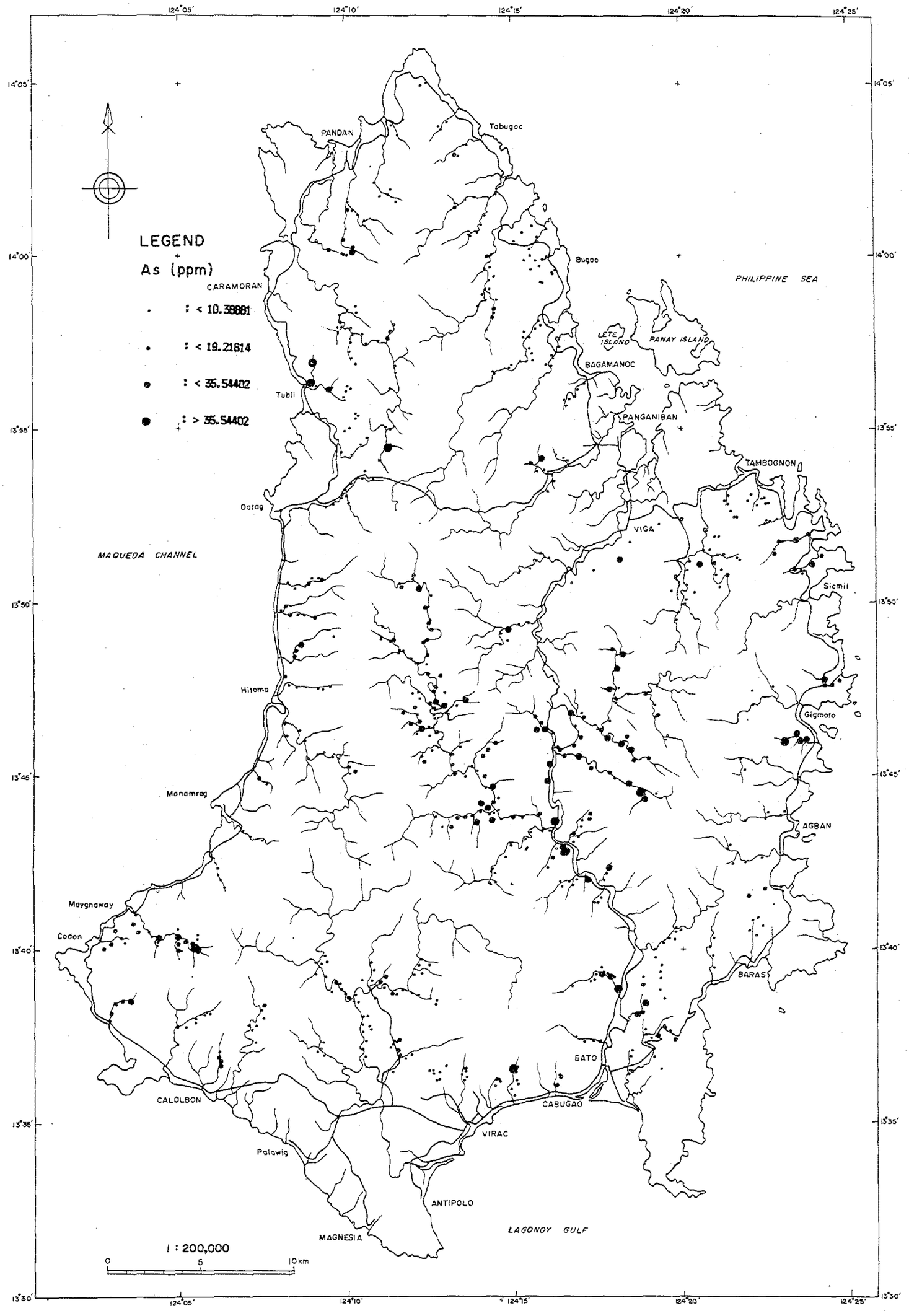

Fig.27 Geochemical Anomaly of Stream Sediments (3)

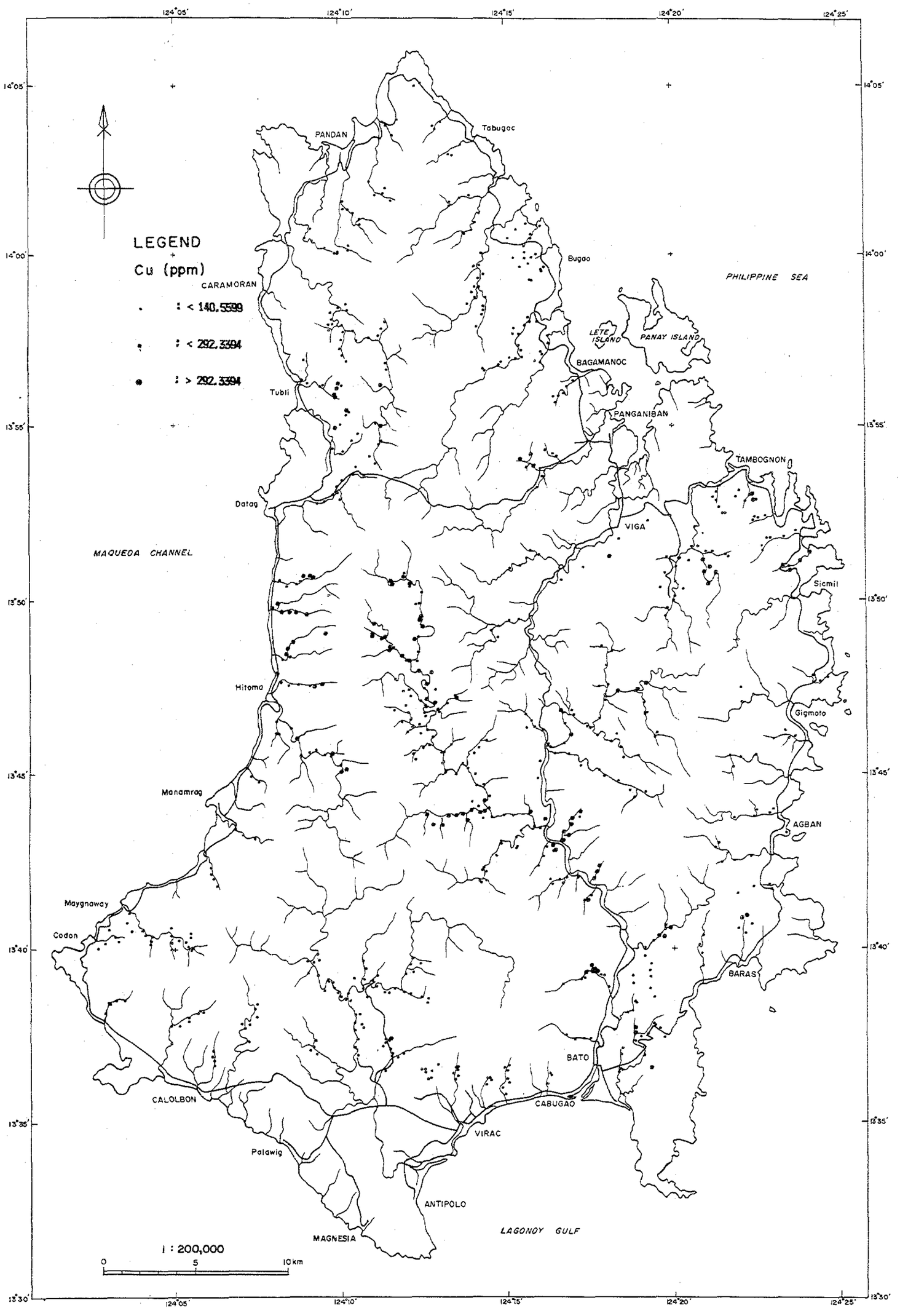

Fig.27 Geochemical Anomaly of Stream Sediments (4)

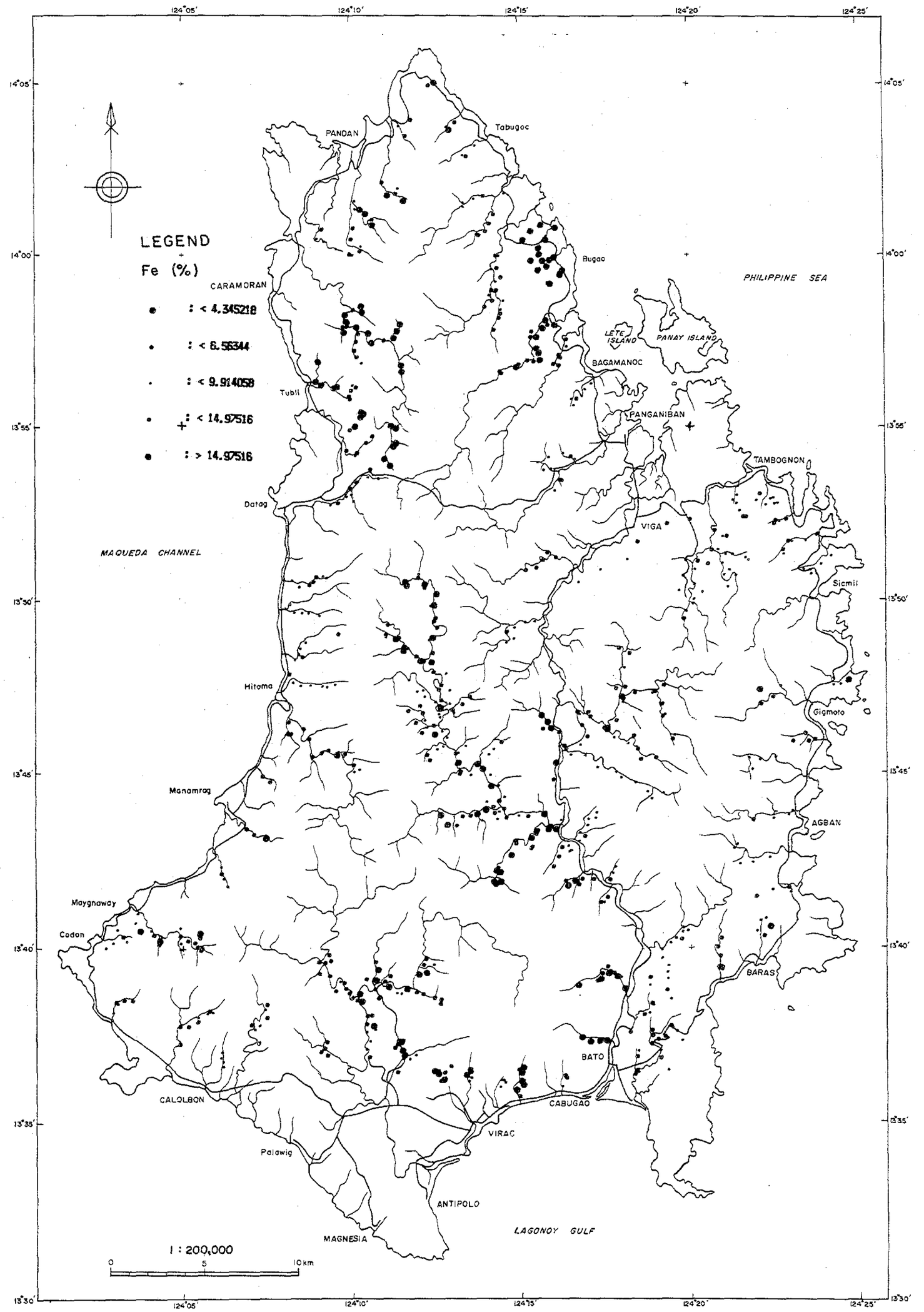

Fig.27 Geochemical Anomaly of Stream Sediments (5)

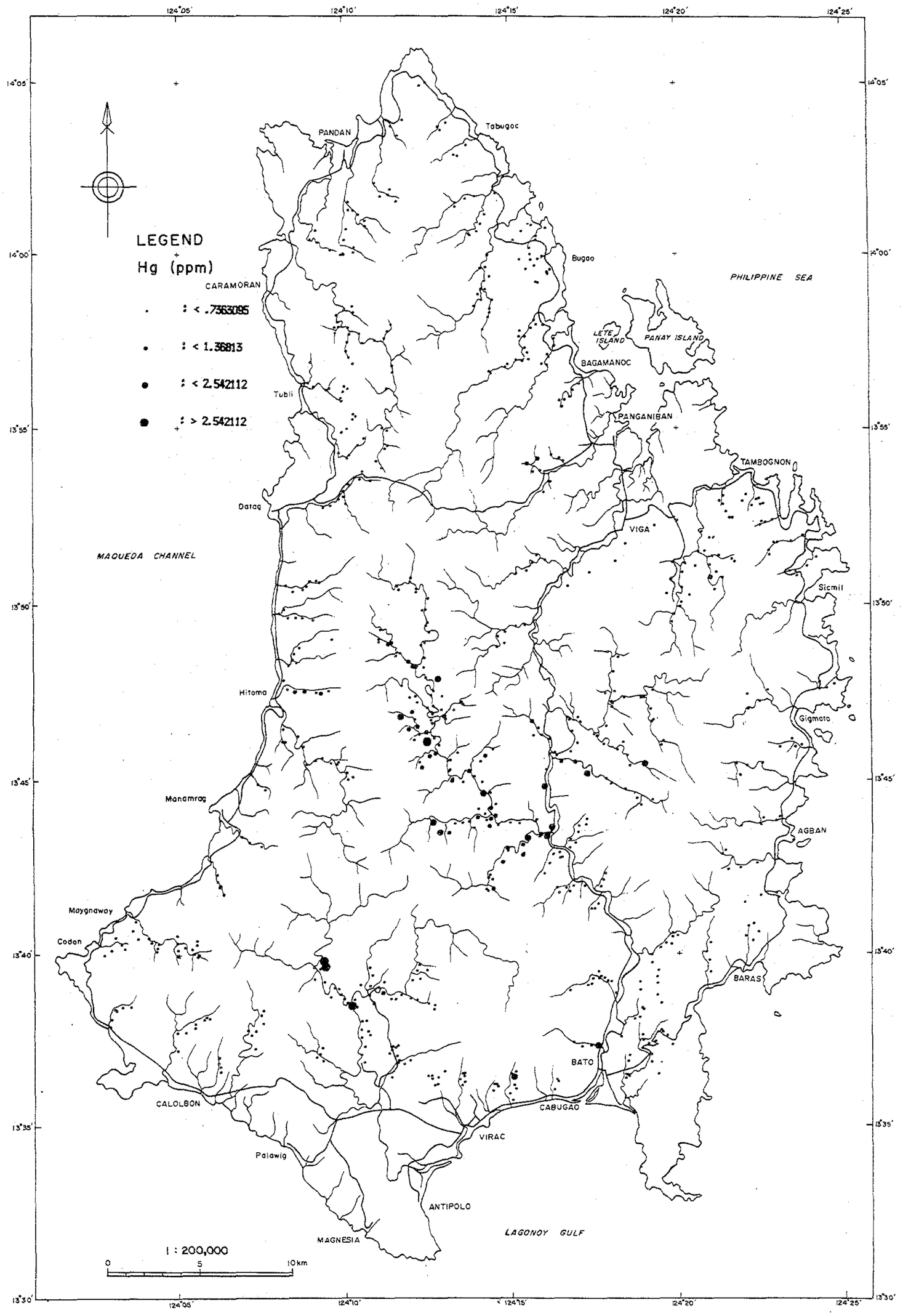

Fig.27 Geochemical Anomaly of Stream Sediments (6)

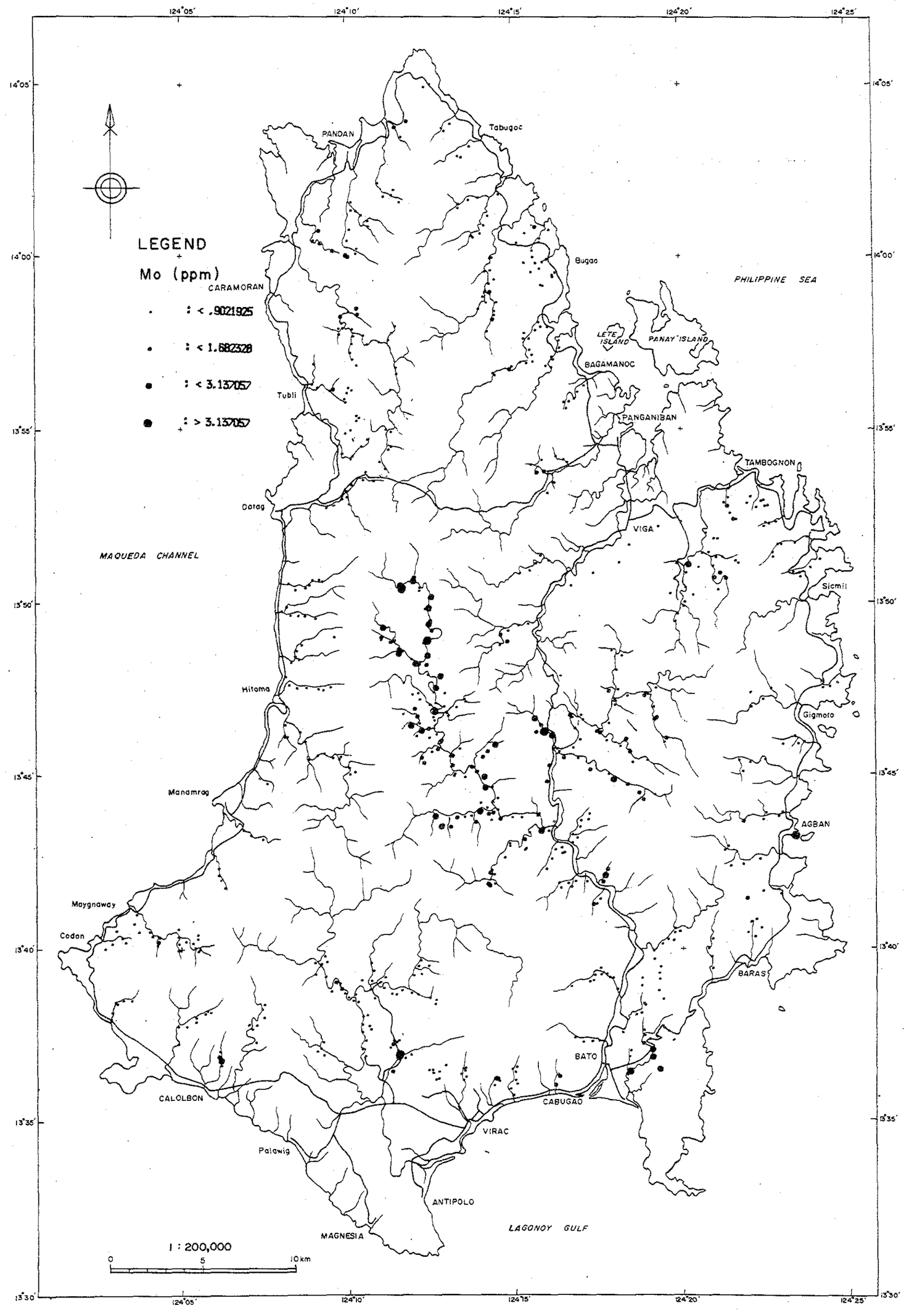

Fig.27 Geochemical Anomaly of Stream Sediments (7)

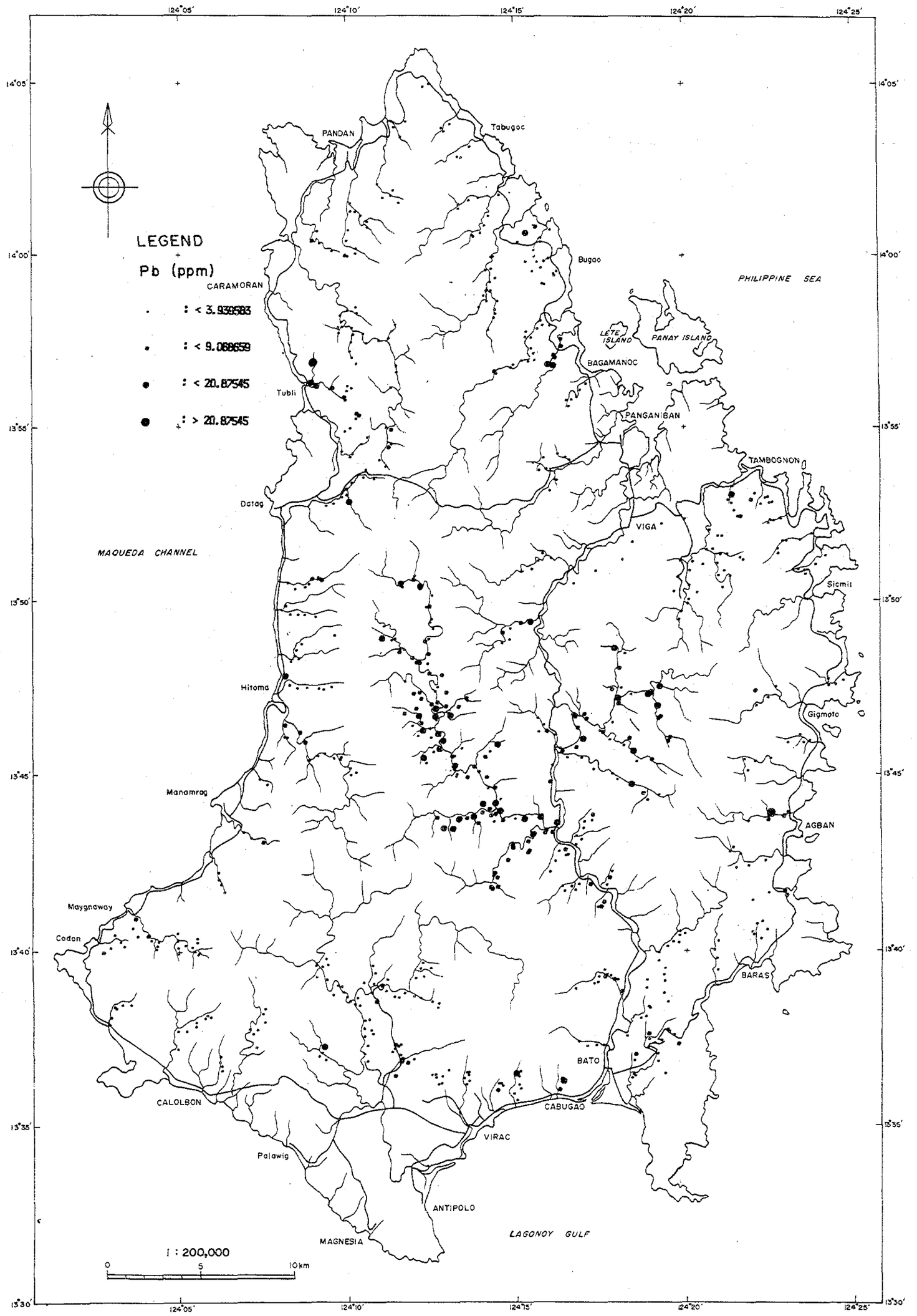

Fig.27 Geochemical Anomaly of Stream Sediments (8)

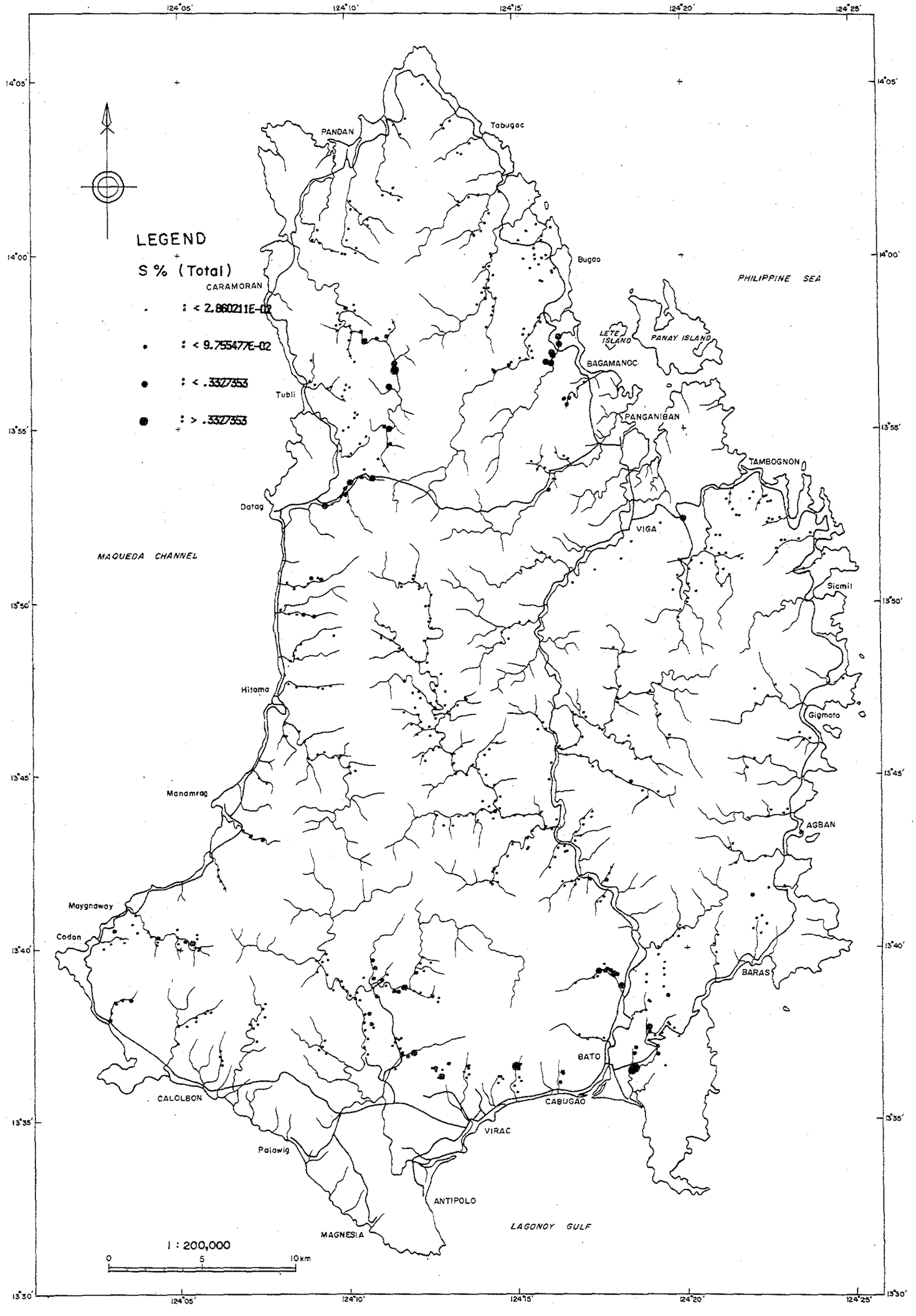

Fig.27 Geochemical Anomaly of Stream Sediments (9)

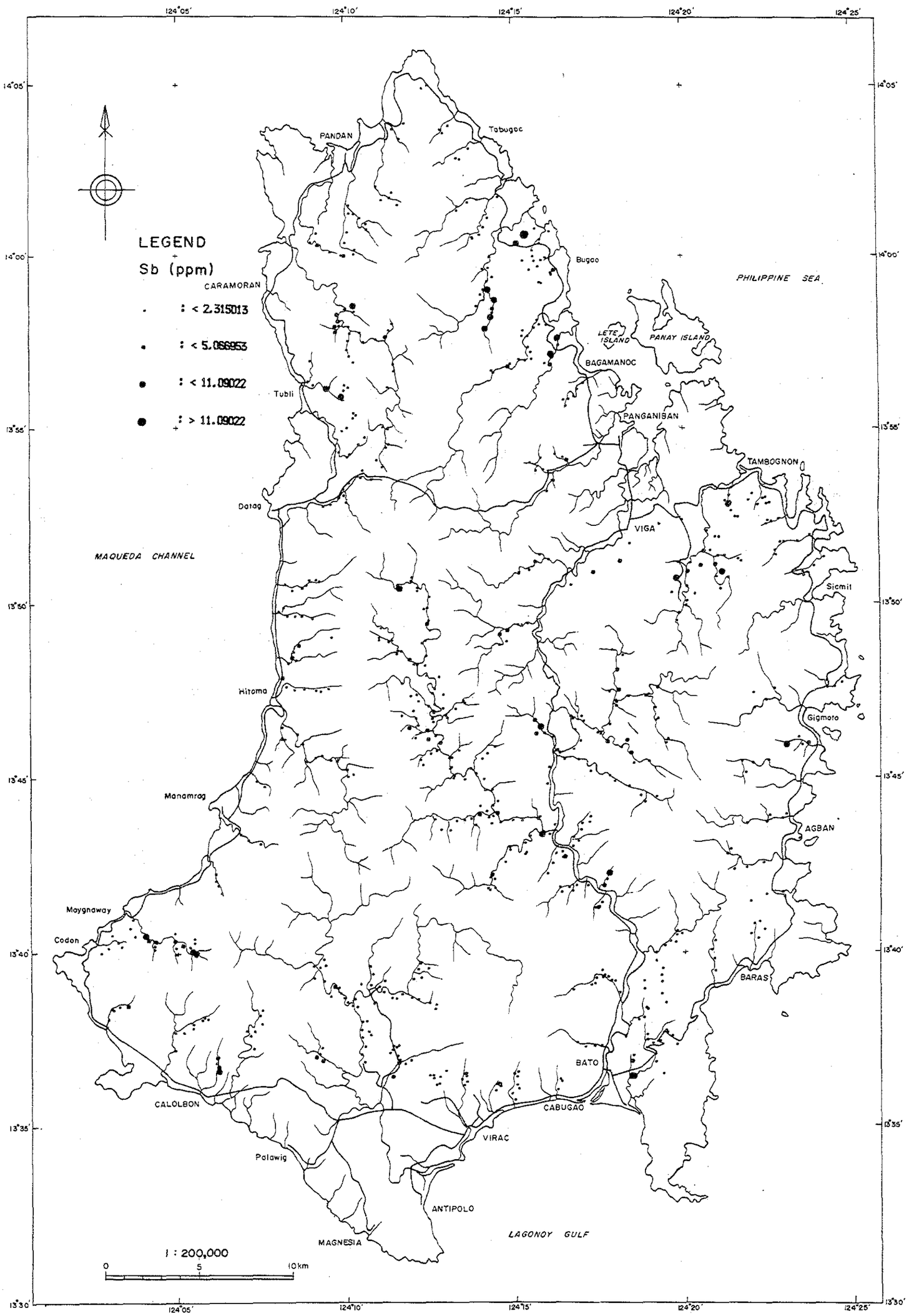

Fig.27 Geochemical Anomaly of Stream Sediments (10)

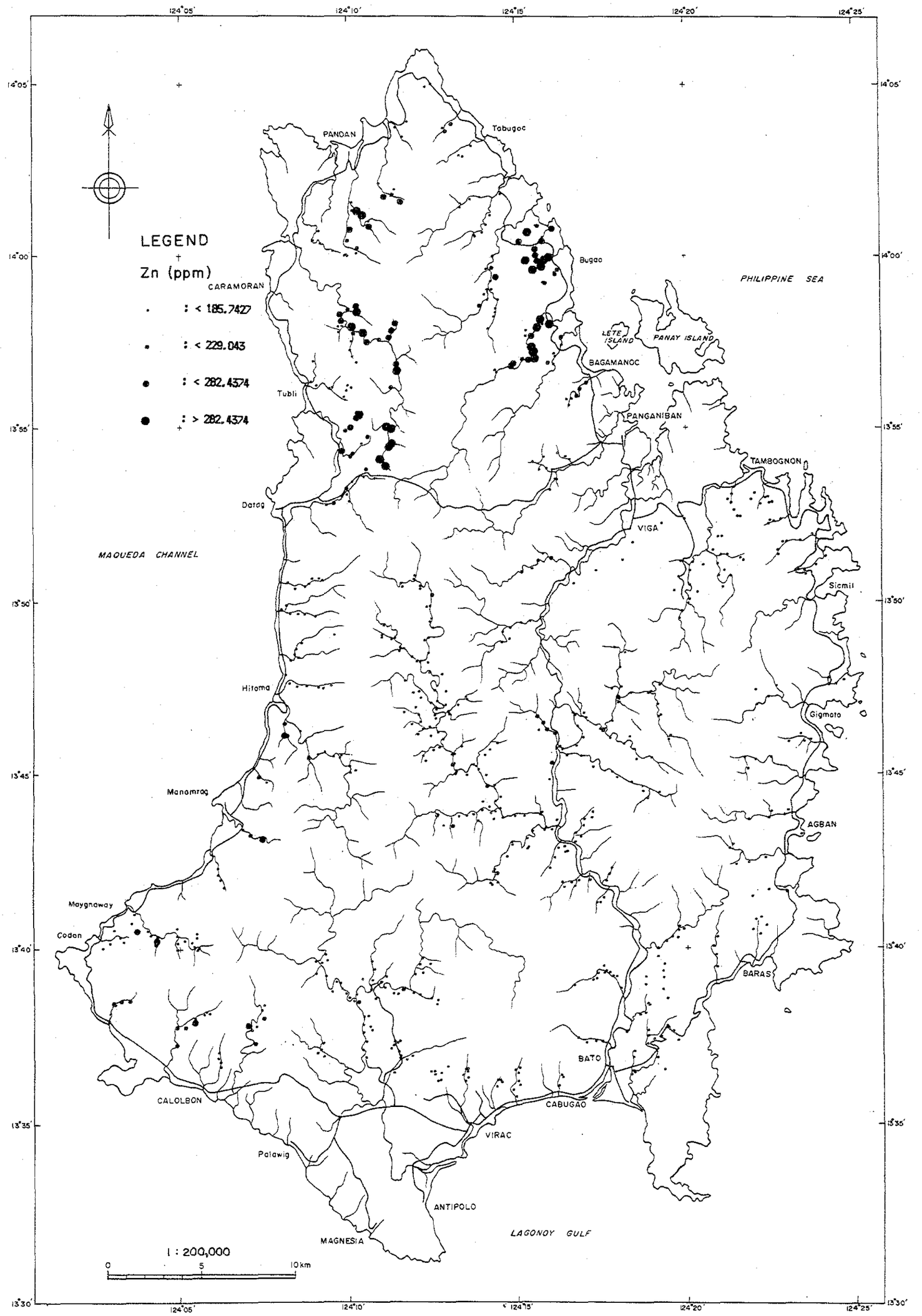

Fig.27 Geochemical Anomaly of Stream Sediments (11)

vicinities.

2-5-5 Principal Component Analysis

Principal component analysis (PCA) was accomplished in order to see if there are groups of elements in their behavior and what control their grouping.

In calculation of PCA, correlation coefficients of Table 26 were used. The result of the analysis is shown in Table 28 and principal component score distributions are shown in Fig.28.

Table 28 **Results of PCA (Stream Sediments)**

Eigen value				Factor Loading					
P.C.	E.V.	Cont.	CumCon		Z-01	Z-02	Z-03	Z-04	Z-05
Z-01	1.863	16.933	16.933	Pb	0.645	-0.077	-0.244	-0.048	-0.042
Z-02	1.807	16.430	33.364	Mo	0.588	-0.091	-0.145	0.199	-0.075
Z-03	1.335	12.137	45.500	Cu	0.559	-0.263	-0.042	0.317	0.271
Z-04	1.050	9.549	55.049	Zn	0.259	0.850	0.165	0.043	0.018
Z-05	1.028	9.347	64.396	Fe	0.277	0.834	-0.029	0.258	0.153
Z-06	0.970	8.821	73.217	Ag	-0.246	0.067	0.753	0.158	0.259
Z-07	0.857	7.786	81.004	As	0.489	-0.398	0.503	0.057	0.222
Z-08	0.690	6.270	87.274	Sb	0.396	-0.205	0.476	0.325	-0.298
Z-09	0.677	6.156	93.429	S	0.021	-0.198	-0.293	0.731	-0.234
Z-10	0.503	4.576	98.005	Au	-0.333	-0.243	-0.175	0.412	0.603
Z-11	0.219	1.995	100.000	Hg	0.277	0.051	-0.249	0.045	0.548

P.C.: principal component, E.V.: eigenvalue, Cont.: contribution ratio, CumCon: cummulative contribution

No conspicuous correlation was observed in Table 26 except for that of Fe and Zn. Likewise no conspicuous principal component is shown in Table 28. Eigenvalue and contribution ratio of first principal component are only 1.86 and 16.9% respectively. Eigenvalues of first six principal components are nearly or over 1.0. This means there is no principal component which explains the behavior of many elements. Each element has the character as shown below.

First Principal Component : Pb, Mo, Cu, (As, Sb) show relatively large factor loadings. This component seems to explain Cu mineralization. But this does not mean strong geochemical anomalies because the assay values for these elements are not so high and the contrasts between high values and low values are not striking. These elements except Cu are more abundant in acidic rocks and shale rather than in basic rocks. In Fig. 28 a high score anomaly zone is distributed in the upper reaches of the Kaglatawan River, where Cu mineralization is reported to have occurred (Angeles et al., 1983). But other high score anomaly zones seem to have no

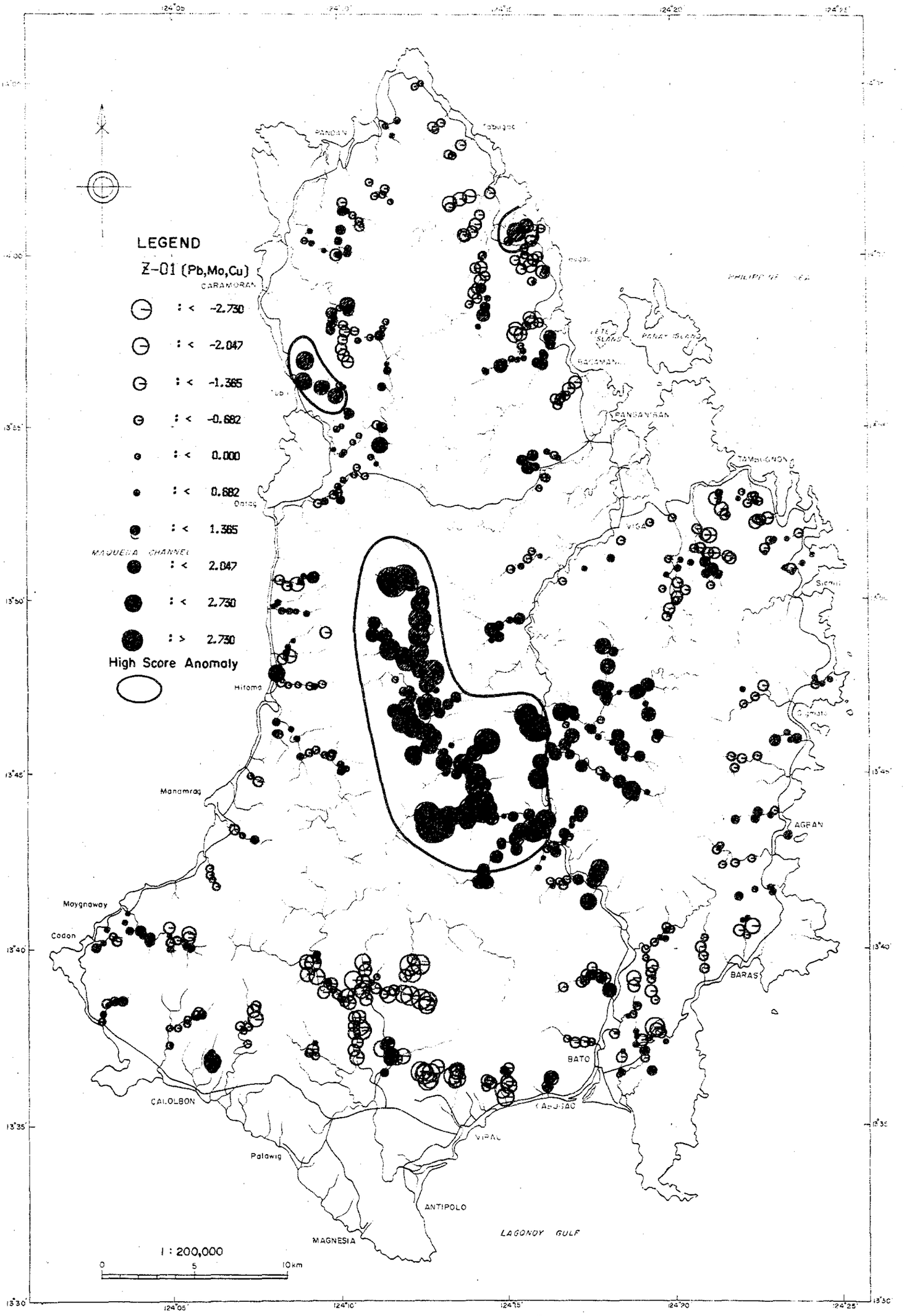

Fig.28 Distribution of PCA Scores (stream sediments)(1)

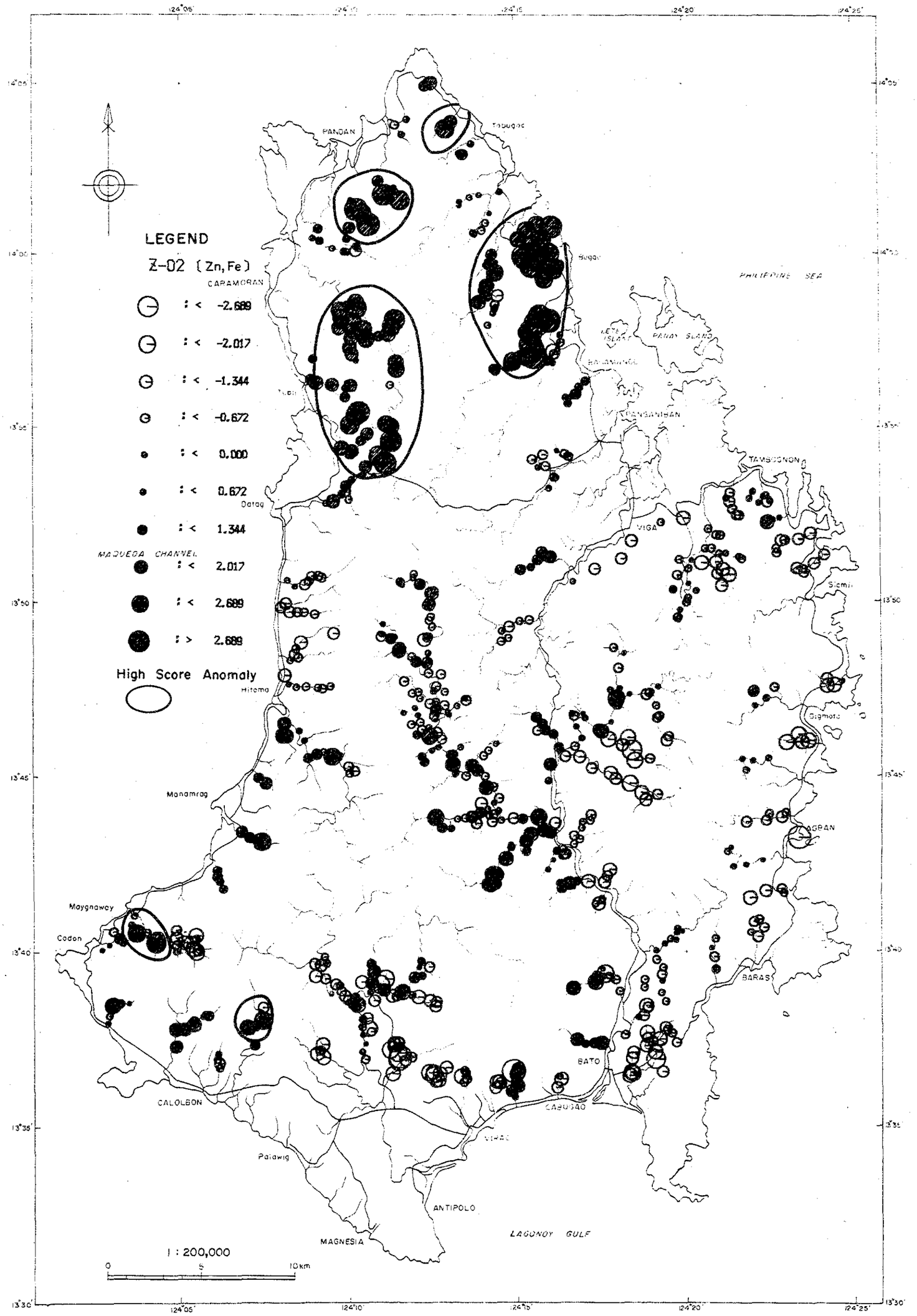

Fig.28 Distribution of PCA Scores (stream sediments)(2)

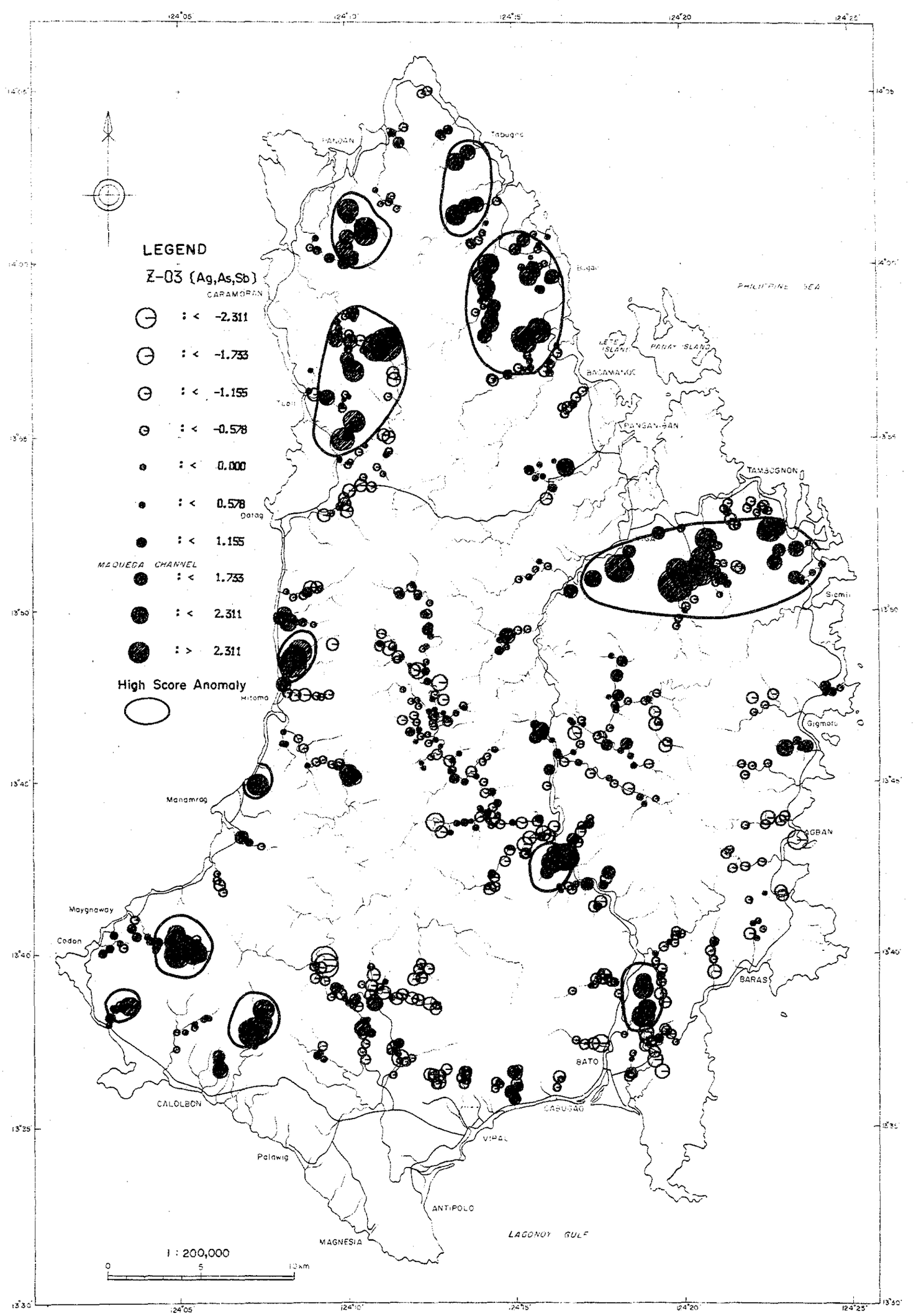

Fig.28 Distribution of PCA Scores (stream sediments)(3)

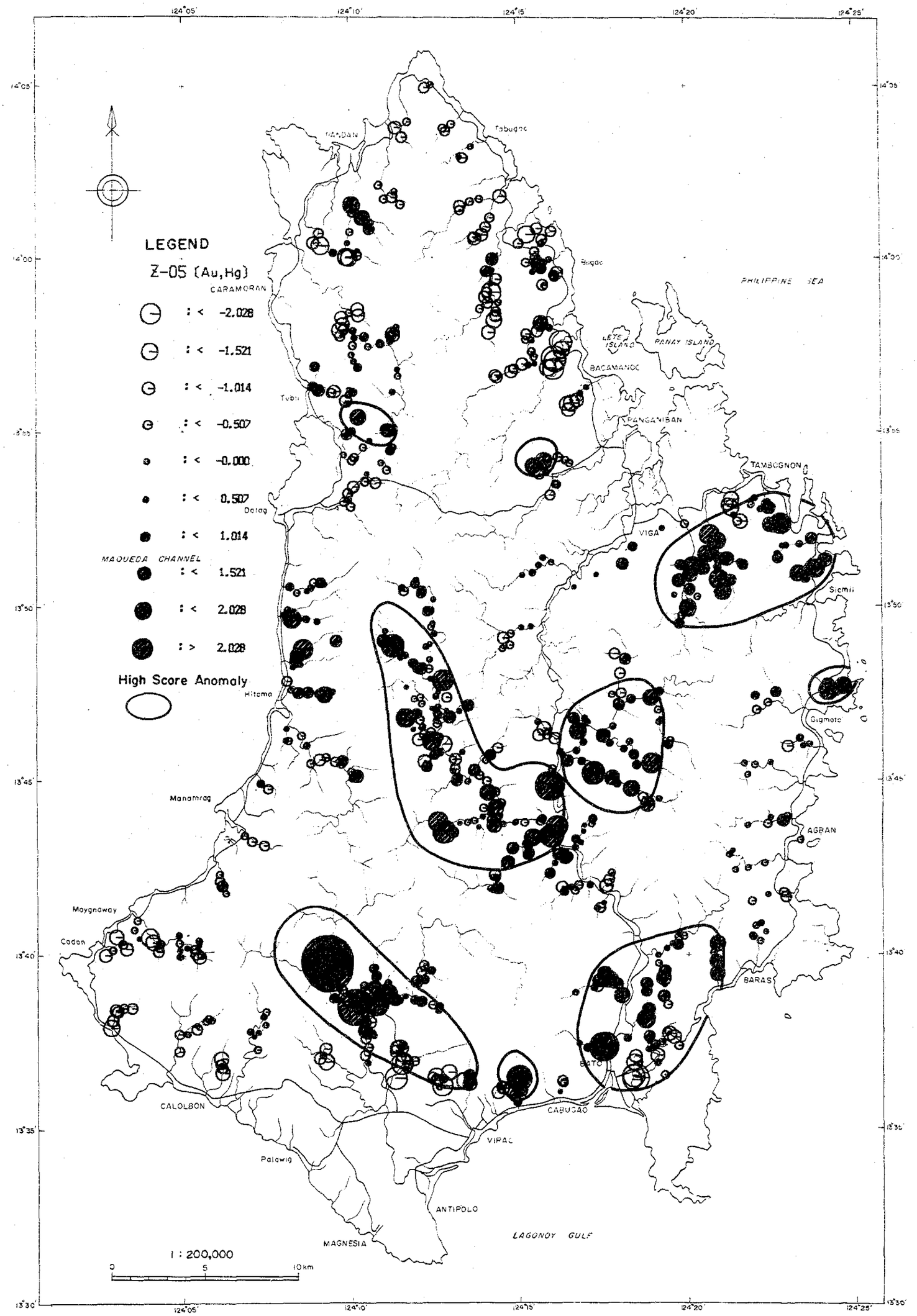

Fig.28 Distribution of PCA Scores (stream sediments)(4)

relation with Cu mineralization. The distributed of these anomaly zones are restricted to the central area of the island occupied by the Catanduanes Formation and intrusive rocks of the Batalay Intrusives. This means the distribution of the high score anomaly zones is controlled by the geology of the area. Therefore both Cu mineralization and geology of the area are shown in the first principal component.

Second Principal Component: Factor loadings of Fe and Zn are large in this principal component. These two elements are abundant in basic rocks and high score anomaly zones are distributed mainly in the area where basaltic rocks of the Yop Formation expose. So second principal component is thought to explain the distribution of basaltic rocks.

Third Principal Component: Ag, As, (and Sb) shows relatively large factor loadings. These elements are related to the mineralization of Au although Au itself is not included in this group. Therefore this principal component is thought to show the peripheral alteration of Au, Ag mineralization. In Fig. 28 the distribution of high score anomalies coinsides with Carorongan Mineral Occurrence and Libjo Mineral Occurrence. Other anomalies are distributed in the area underain by the Yop Formation in the Northern Block.

Fourth Principal Component: S (and Au) show relatively large factor loadings.

Fifth Principal Component: Au and Hg show large factor loadings. Au is related to both fourth and fifth principal components and Au mineralization is thought to be explained in these components. High score anomalies coinside with known Au or Cu Occurrences, i.e. Carorongan, Dugui Too and Libjo Mineral Occurrences (Fig. 28). On the other hand there are some other anomaly zones where mineralization has not been reported yet. High score anomaly shown around Pagsagnahan Village may show the potential for another Au mineralization.

Third, fourth and fifth principal components include factors related to mineralization. First principal component may be thought to include a factor related to Pb, Mo and Cu mineralization. But it seems to show more of the influence of the geology than mineralization, because assay values for these elements are very low. Second principal component shows the distribution of basaltic rocks.

2-6 Discussion

The most conspicuous geochemical anomaly of Au is distributed around Dugui Too Mineral Occurrence. In this area, S and Ag anomalies overlap the Au anomaly. High score anomaly of fifth principal component is also distributed in the area in PCA. Therefore this area

is considered to have high potential of Au mineralization on account of geochemical survey. By geological survey, many intrusive bodies of the Batalay Intrusives are found to generate hydrothermal alteration in the area. Quartz veins width of which is 20cm at maximumn are reported to be distributed in this are by Teodoro et al. (1988). Two samples of these quartz veins showed Au contents of 5.02g/t and 4.80g/t. Predominant quartz veins may be found by further investigation of the area.

Second largest geochemical anomaly of Au is distributed in Carorongan Area. Mo, Sb, Cu and Ag anomalies also overlap in this area. According to PCA high score anomaly zones of third and fifth principal components are distributed in this area. Geochemically speaking this area is the most promising area for Au mineralization. Many floats of quartz were observed in this area in geological survey indicating that many quartz veins are distributed here. Samples taken in this area did not show prospecting assay values, but the presence of predominant quartz veins in this area are highly probable. Au, As and Cu anomalies overlap in Tinaga Village east of this area. It is highly probable that Au bearing predominant quartz veins are found in this area including Tinaga Village by further investigation of the area.

The area around intrusive body of the Batalay Intrusives in type locality include many Au and Cu prospects, such as San Pedro, Libjo, Aroyao and Tilod. Au, Ag, As, Cu, Mo and Sb geochemical anomalies are scattered over the area. According to PCA high score anomalies of third and fifth principal components overlap in the area and high potential for Au mineralizarion is indicated. In geological survey quartz floats over 70cm in diameter are found in San Pedro Mineral Occurrence and a sample taken in Aroyao Mineral Occurrence showed Zn content of 2 1.6%. In Agban Mineral Occurrence high grade Cu ore is sampled. Therefore the area mentioned above together with Agban Mineral Occurrence is one of high potential areas.

Au geochemical anomalies are scattered in the mountainous area northeast of Pagsagnahan Village. In the area As, Mo, Pb and Sb geochemical anomalies overlap. No mineralization has been reported from this area yet. Mineralization may be found by detailed geological survey here.

No conspicuous geochemical anomaly zone is observed in around Agban Mineral Occurrence, southeast of the island. But in this place the outcrop of the most predominant Cu bearing quartz veins in the island is found. The veins has high content of Cu although they do not bear Au. More of predominant quartz veins may be found by accomplishing detailed geological survey around the area.

Au, Ag, As, Cu and Sb anomaly zones overlap in the area around Guiamlong River,

northeast of Hitoma Village. Quartz samples taken in Dulangan Mineral Occurrence, the upper reaches of northern tributary to the Guiamlong River showed Au content higher than 20g/t. But the mineralization there seems small in scale and quartz floats are rarely found along the river. So the presence of many quartz veins cannot be expected in this area. The topography of the area is very steep and the cost for development of the deposit will be very high. Therefore it is concluded that economically minable ore cannot be expected in the area.

Au, Ag, As, Cu, Pb, Sb and Zn geochemical anomaly zones overlap in the area between Tubli Village and the middle reaches of the Hilakan River. But samples taken in this area showed low assay values.

Ag, As, Cu, Pb and Pb geochemical anomalies are scattered along the tributary to the Bato River which joins the main stream at Pagsagnahan Village. Especially along the Kaglatawan River these anomalies overlap. But assay values for these elements are low and the contrasts between high values and low values are not striking. PCA indicates that anomalies in this area are affected by the local geology. Only very weak alteration is observed and quartz floats are rare in the area. Therefore anomaly distributed in this area are considered to be the halo of the local geology.

Au, Ag, S, Pb, Sb and Zn geochemical anomalies are scattered around the area between Mabil Village and the Inipan River, northeast part of the island. Large Fe geochemical anomaly zone includes these anomaly zones. Hydrothermal clay zone is distributed in Mabil Village where pyritization is observed in some part. But no quartz float is found in this place and small anomalies are considered to have originated from small alteration zones. Therefore the presence of predominant quartz veins cannot be expected in the area.

After all it is concluded that Carorongan Area, East of Bato Town Area (including Agban Mineral Occurrence), Dugui Too Area, and East of the Bato River Area are the most important areas in Catanduanes Island.

Chapter 3 Lahuy Island

3-1 Method of Survey

Detailed geological survey and rock geochemical survey were accomplished in the known mineral prospects. Soil geochemical survey was accomplished over the whole island.

1 to 5,000 topographic map which was enlarged from 1to 50,000 map was used in the detailed geological survey of the known Villages. The survey result was compiled into 1 to 5,0 00 geological map (PL-17).

1 to 10,000 topographic map which was enlarged from 1 to 50,000 map was used in soil geochemical survey over the whole island. A base line was set up by surveying and the 100 mx200m grid sampling was done. 1kg of B layer soil was sampled as a rule.

Soil samples were dried and sieved to -80 mesh fraction, then divided among the Philippine side and Japanese side. The number of samples taken is 812. Locality of samples is shown in PL-18.

3-2 Geological Survey

3-2-1 General Geology

Torres (1978) described the geology and mineralization of Au prospects in Gata Village. 1 to 50,000 geological map of Gibgos (MGB, 1985) is available.

According to 1 to 50,000 geological map of Gibgos (MGB, 1985), geology of the island comprise Lahuy Formation of late Miocene, Tertiary. But K-Ar dating accomplished on four rock samples in this survey showed the ages between 41.0±1.0Ma and 93.0±3.0Ma, i.e. between the ages of late Cretaceous and late Eocene (Table 29). The age of Lahuy Formation seems to be older than Miocene. If the result of dating is correct, there may be some volcanic activities, not one. In this report the age of Lahuy island is set on late Cretaceous.

Table 29 **K-Ar Dating of Igneous Rocks (Lahuy Island)**

Sample No.	Rock Type	K-Ar Age(Ma)
BLR-001	Dacitic Intrusive	66.8±4.1
BLR-028	Andesitic Lava	88.2±2.8
ALR-071	Andesitic Lava	93.0±3.0
ALR-075	DacitidLava	41.0±1.0

Lahuy Formation is mainly composed of andesitic (dacitic to basaltic) volcanic rocks intercalated with tuffaceous sandstone, shale and conglomerate. Volcanic rock consists of lava,

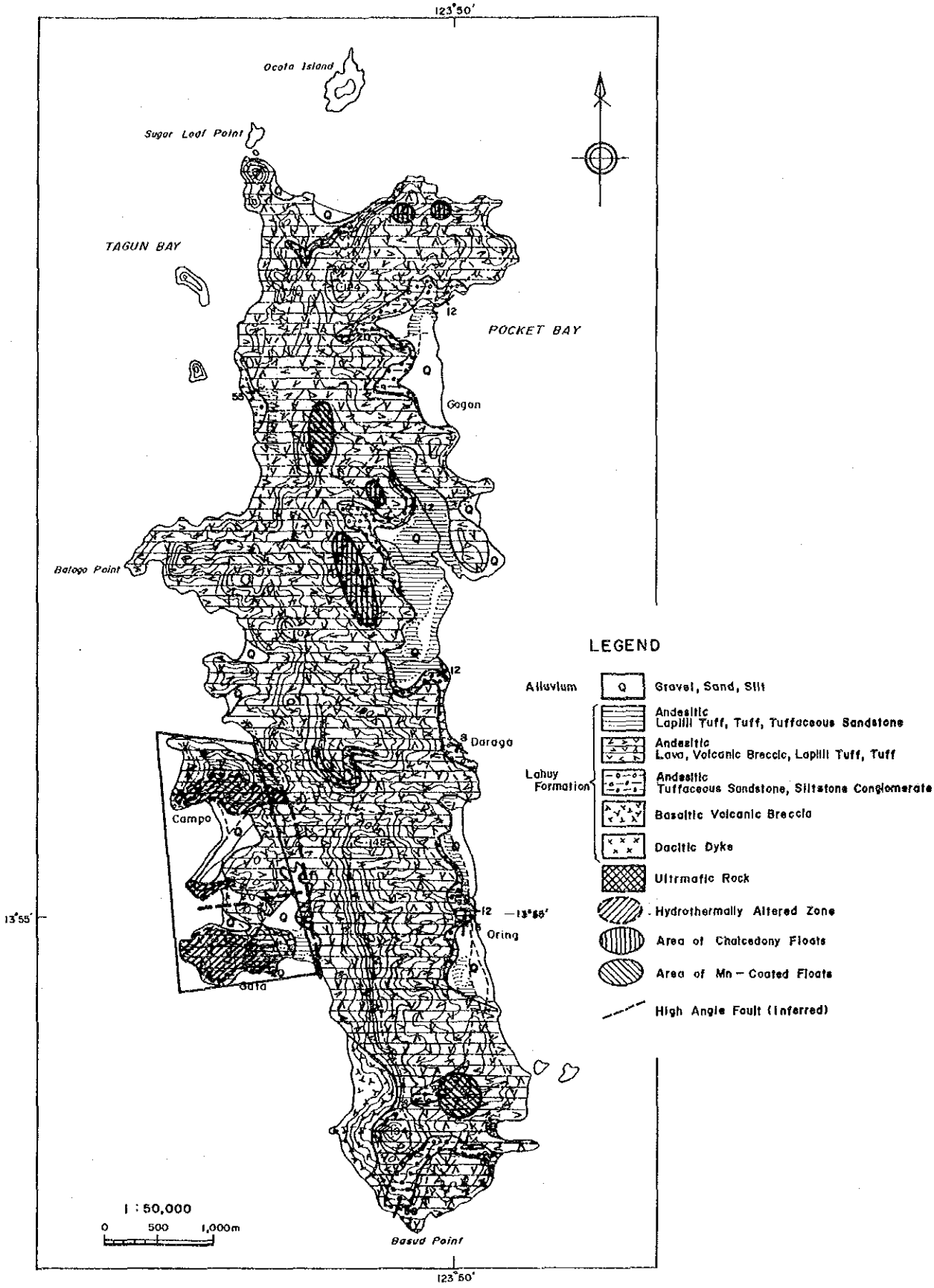

Fig.29 Geologic Map of Lahuy Island

tuff breccia and tuff. Compositionally they are mainly andesitic, but partly dacitic lava and basaltic tuff breccia are observed. Tuffaceous sandstone, shale, conglomerate are intercalated in these volcanic rocks and shows northeast to northwest strike and gentle dip to the east.

Gata Village which is situated in the southwest part of the island has been known to be gold occurring place from 1930s. Lahuy Formation there is subjected to strong hydrothermal alteration. In contrast to this rocks in other area of the island (reconnaissance survey area) is rather fresh. At the east end of the detailed survey area a float of ultramafic rock was sampled. Under the microscope the sample (ALR-058) is mainly composed of olivine and augite with small amount of spinel. Olivine is observed to be intensely serpentinized at its periphery.

Presence of fault is inferedbetween the detailed survey area and the reconnaissance survey area and the western block (the detailed survey area) is thought to be uplifted.

The presence of floats of chalcedonic quartz and secondary coverage of Mn in the reconnaissance survey area imply the occurrence of mineralization underground.

3-2-2 Geology of the Detailed Survey Area

Lahuy Formation of the detailed survey area is composed of four parts. One is made up of tuffaceous sandstone and tuff which is distributed in the southeast part of the area. And another one is andesitic pyroclastic rocks which widely exposes from north to south of the area. Another one is made up of tuffaceous sandstone and conglomerate which exposes at the northwestern part of the area. And the last one is dacitic dyke which cut the first two parts from east of Gata Mineral Occurrence to east of Calising Point. Geology of the area is shown in Fig. 30.

In the southeast part of the detailed area there expose tuffaceous sandstone, lapilli tuff and partly tuff breccia which strike to northeast and dip gently to southwest. These rocks are grey to greenish grey in color and subjected to hydrothermal alteration along fractures. They comformably overlie andesitic pyroclastic rocks which exposes on their north. Andesitic pyroclastic rocks consist of lava and tuff breccia. At Calising Point, the central part of the area, andesitic lava shows conspicuous flow structure. Along coast lava and tuff breccia are relatively fresh and show greenish gray color. But they are strongly altered around gold prospects and become white.

Along northern slope of the hill east of Calising Point there are at least two cycles of tuff breccia and lava. these sequence show strike of NNW and dip steeply to the east.

At west of Campo, northwest part of the area, greenish gray colored altenated beds of

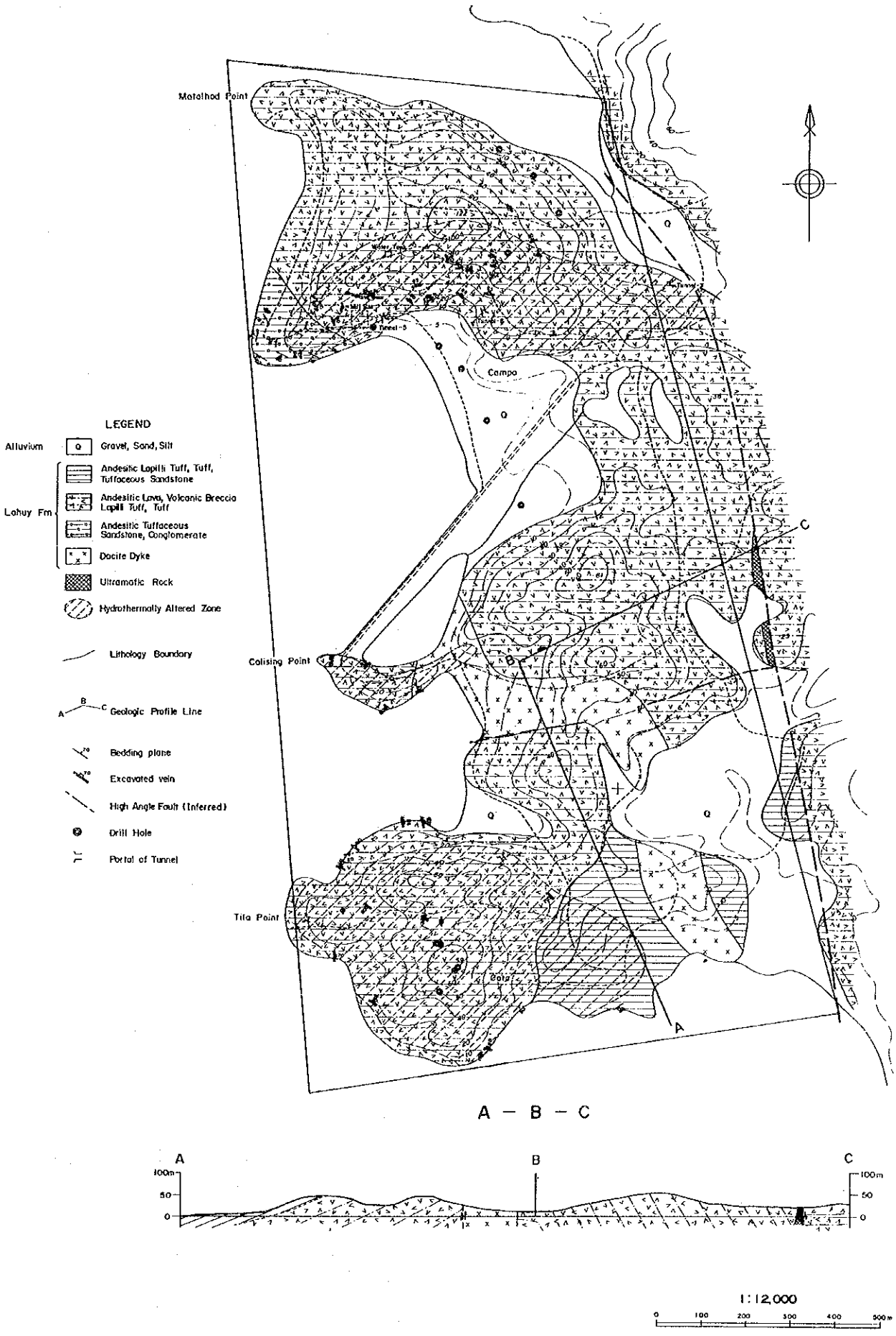

Fig.30 Geologic Map of the Detailed Survey Area

tuffaceous sandstone and conglomerate are exposed. They show NW strike and dips almost vertically. At Campo Mineral Occurrence rocks are too intensely altered to identify the rock type, but along northern coast of Campo Mineral Occurrence andesitic lava exposes.

Under microscope andesite (BLR-064) shows porphyritic texture. The groundmas is composed of plagioclase, hornblende, pyroxene, glass and opaque minerals. Phenocrysts consist of plagioclase, hornblende and pyroxene and they are calcitized and sericitized to some extent.

From the east of Gata Mineral Occurrence to the east of Calising Point a dacitic dyke cuts through andesitic pyroclastic rocks, tuffaceous sandstone and lapilli tuff. Megascopically this rocck looks rather fresh and shows dark green color and has porphyritic texture with phenocrysts of feldspar, amphybole, quartz. But at the east of Calising Point the dyke is observed to be hydrothermally altered and become white.

Under the microscope the dacite (BLR-001) has phenocrysts of plagioclase, hornblende, K-feldspar and opacitic periphery is observed around hornblend crystals. Fine crystals of opaque mineral scatter in the groundmass.

3-2-3 Geologic Structure of the Detailed Survey Area

As mentioned before in southeastern part of the area Lahuy Formation shows NE strike and dips gently to SE, whereas in north and central part the formation shows NWto NNW strikes and vertical to steep dips to the east. The presence of a EW trending fault is inferred between the north to central part and the south part and the dacitic dyke may have intruded partly along the fault.

Ultramafic rock sampled at the east end of the detailed survey area implies the presence of a NS trending fault by which the western block (the detailed survey area) is uplifted.

3-2-4 Ore Deposit and Mineralization

There was active mining activities at Campo and Gata Mineral Occurrences before the Second World War and after the war several times of exploration were done on the area. Now local people are doing small scale mining in this area.

The rock around Gata Mineral Occurrence, Campo Mineral Occurrence and Calising Point is intensely altered and there are many tunnels and pits and trenches in these places. The ore accompanies quartz and clay veins. At Gata Mineral Occurrence NS to NW to EW trending veins are dominant whereas at Campo Mineral Occurrence EW to NW trending veins are

dominant. Veins swell to 30cm and pinch to 5cm at the interval of 2m. Quartz veins accompany galena, sphalerite, chalcopyrite, pyrite and amethyst . According to local people if galena and sphalertite and amethyst accompany the ore, the ore tends to be rich in Au. Sphalerite is clear with low content of Fe.

Under the microscope ore consists of pyrite, sphalerite, chalcopyrite and galena with gangue minerals such as quartz, calcite and K-feldspar. Gold is observed along boundaries of gangue minerals and pyrite crystals (BLR-10-8, BLR-10-10-2), in pyrite crystals (BLR-10-10-2), and in sphalerite crystals (BLR-24-1). Galena is sometimes observed to be included in pyrite crystals (BLR-10-10-2) and Sphalerite (BLR-24-1). Also, chalcopyrite is sometimes included in sphalerite crystals. Sphalerite is pale yellow at its center, and becomes colorless at the periphery, showing zoning in Fe content (BLR-24-1).

Ore assay results are shown in Table 7 in the appendix. The maximum assay value for Au is 46.8g/t and minimum value is <0.03g/t. The average of assay values for Au is 6.0g/t. Among the 23 samples assayed, those showed high contents of Au are also high in Ag, Cu, Pb, S and Zn contents.

(1) Powder X-ray Diffraction

53 samples taken in the detailed survey area were submitted to X-ray diffraction. The results are shown in Table 6 in the appendix. Distribution frequencies of alteration minerals are checked with respect to the alteration degree of the rock samples. The alteration degree of the rock is megascopically evaluated as shown in Table 30.

Table 30 **Alteration Degree of Rock Samples**

Alteration Degree	Megascopic Characters
0	Fresh
1	Rock texture is clear with minor argillization of mafic minerals
2	Rock texture is a little bague with milky feldspar.
3	Rock becomes white with bague rock texture
4	Rock is white with little trace of rock texture
5	White rock with no trace of original texture
6	Clay and quartz vein, Ore

In calculation of frequency of minerals, the amount of minerals which is evaluated from quartz index is used. The amount of minerals, abundant, common, small amount, rare, are made into numerical values as 4, 3, 2, 1, 0 respectively. These values are totaled for each

alteration degree and each alteration mineral. Then frequency of an alteration mineral is got by dividing the total value by the number of rock samples of the alteration degree.

Frequency of mineral A in alteration degree N
= Σ(Amount of mineral A) / Number of samples in alteration degree N

Frequency distributions of alteration minerals are shown in Fig. 31

Fig.31 Frequency Distribution of Alteration Minerals

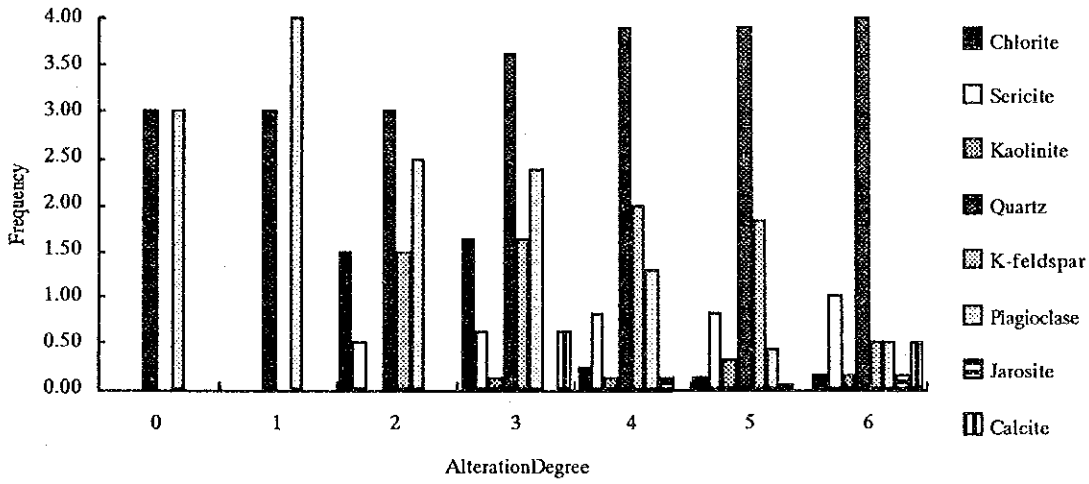

As the alteration degree increases, plagioclase decreases, and K-feldspar, quartz, sericite increases. Chlorite appears at the first stage of alteratio but decreases as the alteration degree increases. The alteration of the area is characterized by increase of quartz, K-feldspar, and sericite.

(2) Homogenization Temperature of Fluid Inclusion

Homogenization temperatures of 23 quartz samples taken in the detailed survey area were measured. In measurement Metror FP5 (temperature control unit) and FP52 (heating stage) were used and the temperature when a gas bubble extincts is measured with accuracy of 0.1 degree Celsius.

Many fluid inclusions are observed in quartz and amethyst crystals but there are some samples in which no inclusion is observed. Fluid inclusions in milky quartz crystals which are observed among ore minerals are too small (less than 1μm in diameter) for the measurement. The number of samples homogenization temperatures were measured is 6 although small

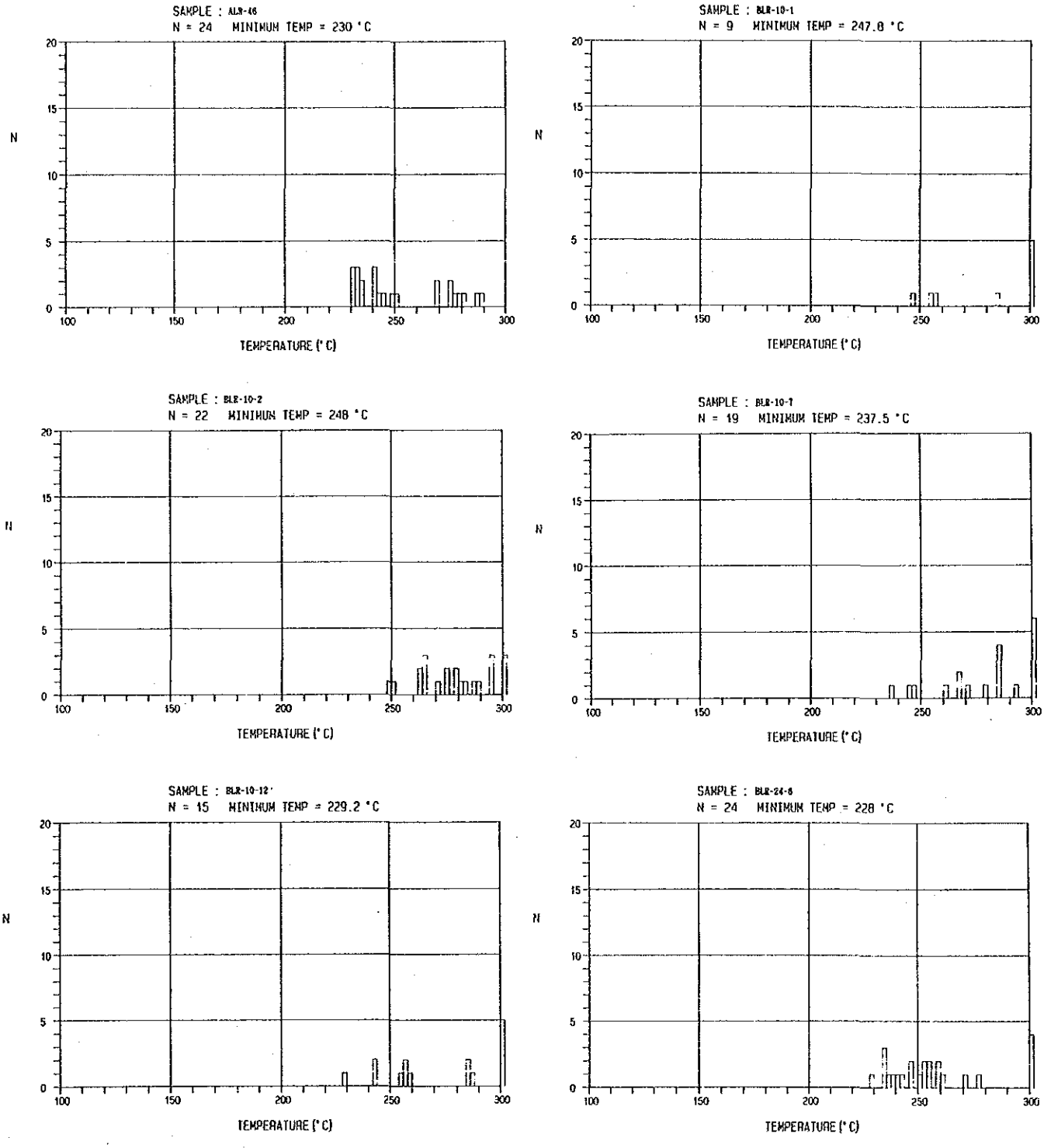

Fig.32 Frequency Distribution of Homogenization Temperature

inclusions of nearly 1μm was measured.

The result of the measurement is shown in Table 31.

The sizes of fluid inclusions the homogenization temperatures were measured are between 1x2μm and 40 x 70μm. The homogenization temperatures range from 228°C to more than 300° C. The average temperature is 271.3°C. The homogenization temperature of inclusions which showed the temperature more than 300°C were treated as 315°C in calculation of the average temperature, because their gas phase is almost at the point of extinction at 300°C.

Table 31 **Homogenization Temperature of Fluid Inclusions**

Sample No.	Tested Mineral	Inclusions	Number	Average	Range
ALR-013	Quartz	No inclusion			
ALR-040	Calcite	No inclusion			
ALR-040-1	Calcite	No inclusion			
ALR-046	Quartz	Measured	24	252.7	230.0-288.3
BLR-010-1	Amethyst	Measured	9	291.2	247.8->300
BLR-010-2	Quartz	Measured	22	280.3	248.0->300
BLR-010-3	Quartz	No inclusion			
BLR-010-4	Amethyst	Too small inclusions			
BLR-010-5	Quartz	No inclusion			
BLR-010-6	Quartz	No inclusion			
BLR-010-7	Quartz	Measured	19	283.9	237.5->300
BLR-010-11	Quartz	Too small inclusions			
BLR-010-12	Amethyst	Measured	15	278.3	229.2->300
BLR-024-1	Amethyst	Too small inclusions			
BLR-024-2	Amethyst	Gas inclusion			
BLR-024-3	Amethyst	Gas inclusion			
BLR-024-4	Quartz	No inclusion			
BLR-024-5	Quartz	No inclusion			
BLR-024-6	Amethyst	Measured	24	259.7	228.0->300
BLR-024-7	Quartz	Gas inclusion			
BLR-024-8	Quartz	Gas inclusion			
BLR-026	Quartz	No inclusion			
BLR-053	Quartz	No inclusion			

Fluid inclusions are classified into two groups. One is relatively large inclusions which are distributed at randum in crystals and thought to be primary in origin. Another one is aligned along cracks and thought to be secondary in origin. Temperature of fluid inclusions of 4 samples showed two seperate distributions, one is between 230°C and 270°C, another one is around 270°C and 300°C. Secondary inclusions are observed more in the former group while more of primary inclusions are observed in the latter. There are two samples which show

continuous distribution of homogenization temperatures from 230°C to over 300°C. In these samples primary inclusions and secondary inclusions are thought to have been formed continuously.

There are 1 to 50μm sized inclusions in the extensions of planes where secondary inclusions are distributed. Liquid phase is hard to distinguish and no phese change was observed upon heating in these inclusion. Therefore these inclusions are thought to have only gas phase. More of these gas inclusions are observed in quartz and amethyst crystals which are in paragenic relation with ore minerals, implying the causal relation of occurrence of boiling and precipitation of ore minerals.

Homogenization temperatures of fluid inclusions show the range between 228°C and more than 300°C. This means temperature went down from over 300°C to 228°C in hydrothermal activity. If so, the pressure of single phase hot water went down from 87.6atm to 27.5atm by 60.1atm. This corresponds to the drop of ground water level by 601m. Therefore erosion of 601m was occurred during the crystal growth of quartz and after hydrothermal activity ceased, another 285m of erosion is considered to have occurred.

(3) Measurement of Resistivity and Polarization

Total of 25 rock samples were submitted to measurement of resistivity and polarization. Before measurement of resistivity and polarization, samples were cut and formed into rectangular prism of 5cmx5cmx10cm, then kept soaked in distilled water for one week. For measurement IP and Resistivity Core Tester CT-1 of Phoenix Geophysics Limited was used. Because of the property of the apparatus, measurement of polarization was done at frequencies of 0.3Hz and 5Hz. Table 32 shows the result of measurement. Rock samples were classified according to the alteration degree which is mentioned in 3-2-4(1). Resistivity and Polarization of the rock samples showed the ranges of 42 to 994Ω ·m (average 273Ω ·m) and 1.4 to 8.7% (average 4.4%) respectively.

Frequency distribution of resistivity values for each alteration degree is shown in Fig. 33. Because of the lack of abundance in number of samples, samples are classified by modified three stages of alteration degrees, i.e. alteration degree 0 to 1, 2 to 3 and 4 to 6. Frequency was divided by the number of samples of the alteration degree in order to decrease the effect of difference in number of samples.

Table 32 **Resistivity and Polarization of Rock Samples**

Sample No.	Description	Alt.Deg.	Res.(Ω·m)	Pol.(%)
ALR-014	Hydro. Alt. Rock (silicified, argillized)	5	79	3.6
ALR-017	Hydro. Alt. Rock (weakly tex.remains)	4	122	3.0
ALR-021	And. Pyroclastic Rock (hard)	1	601	4.5
ALR-022	And. Pyroclastic Rock (weak hydro. alt.)	3	74	3.1
ALR-026	Hydro. Alt. Rock (no tex. remains)	4	111	2.9
ALR-032	And. Tuff (weak hydro. alt.)	3	994	1.9
ALR-039	And. Tuff (weak hydro. alt.)	3	96	4.4
ALR-042	Tuff (hydro. alt., weathered)	3	100	3.6
ALR-044-2	Hydro. Alt. Rock (cgl. or tuff breccia)	4	46	3.8
ALR-052	Hydro. Alt. Rock	5	154	3.8
BLR-001	Dacite (Fresh)	1	340	6.4
BLR-006	Hydro. Alt. Rock	5	69	3.0
BLR-033	Tuff Breccia (weak hydro alt. Chl.)	3	47	2.5
BLR-034	Au Ore (Panique Tunnel)	6	336	8.7
BLR-043	And. Lava (Fresh, Panique Point)	1	256	5.0
BLR-079	And. Tuff (weakly weathered, hard)	2	680	1.4
BLR-107	And. Pyroclastic Rock (Fresh)	1	170	2.3
BLR-111	And. Lava (weakly weathered)	2	237	5.1
BLR-119	And. Lava (Fresh)	1	580	3.9
BLR-125	And. Pyroclastic Rock (weakly weathered)	2	239	7.8
LAE-03R	And. Pyroclastic Rock (weathered)	3	303	7.3
LAE-12R	And. Lava (weakly hydro. alt.)	3	344	7.2
LAE-009	Hydro. Alt. Rock	5	42	8.1
LA-25-12R	And. Pyroclastic Rock (weathered)	3	89	3.6
LA-43-10¯11R	Basaltic Lava (relatively fresh)	1	716	3.8

Abbrebiations alt.deg.: alteration detree, res.: resistivity, pol.: polarization, hydro. alt.: hydrothermally altered, and.: andesitic, tex.: texture, chl.:chloritized

Fresh rocks (alteration degree 0 to 1) show wide range of resistivity of 170 to 716Ω·m, average being 443Ω·m. But 50% of fresh rocks show high resistivity values of more than 500Ω·m. Rocks of alteration degree of 2 to 3 also show the wide range of resistivity distribution from 47Ω·m to 994Ω·m, average being 291.2Ω·m. But there is a tendency that as resistivity becomes higher the frequency of rocks classified as alteration degree of 2 to 3 gradually becomes lower in Fig. 31. Rocks which is classified as alteration degree of 4 to 6 show relatively low resistivity values between 42Ω·m and 336Ω·m, average being 119.9Ω·m. There is a obvious tendency that frequency of rocks classified as alteration degree 4 to 6 becomes lower as resistivity becomes higher.

Fig.33 Frequency Distribution of Resistivity of Rocks

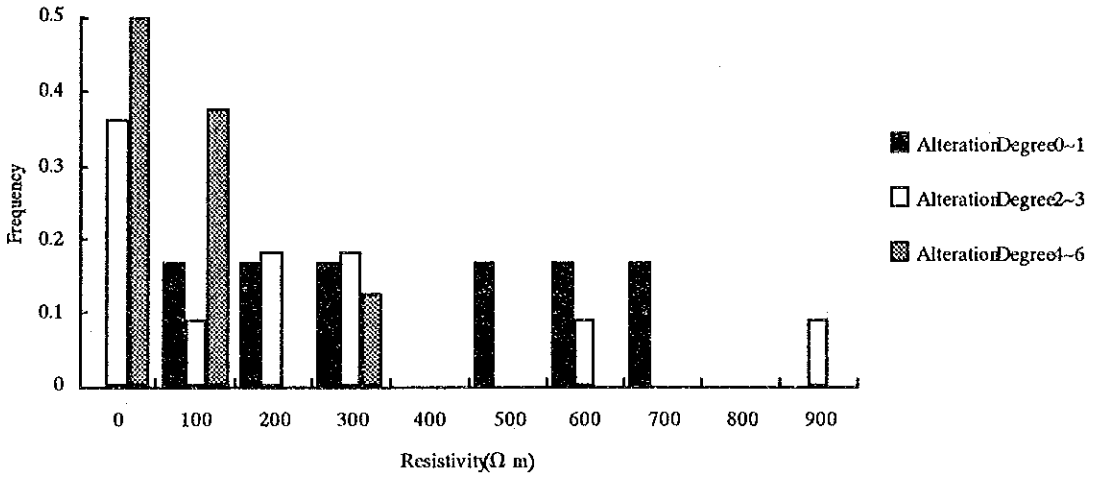

Although the resistivity values are variable in each alteration degree, there is a clear tendency that fresh rocks show relatively high resistivity and altered rocks show lower resistivity.

Fresh rocks submitted to the measurement are one dacite dyke sample, four andesitic volcanic rock samples and one basaltic lava sample. Dacite dyke sample (BLR-001) shows the resistivity of 340Ω ·m, while andesitic rocks show the resistivity ranging from 170Ω ·m to 60 1Ω ·m, average being 401.8Ω ·m and basaltic rock sample shows high resistivity of 716Ω ·m. This cannot be a general tendency because the number of samples is very small, but according to the result, the resistivity became higher with decreasing SiO_2 content.

(3-2) Polarization

Rock samples classified as alteration degree 0 to 1 show polarization ranging from 2.3% to 6.4%, average being 4.32%. Rocks of alteration degree 2 to 3 show polarization ranging from 1.4% to 7.8%, average being 4.35%. Polarization values of rocks classified as alteration degree of 4 to 6 range from 2.9% to 8.7% and the average is 4.61%. Fresh rocks show relatively small variance. But there is no conspicuous difference in average values between different alteration degrees. Frequency distribution of polarization calcurated in the same way as frequency distribution of resistivity is shown in Fig. 34. In every alteration degree, peak frequency lies around 3 to 4% of polarization. There is no tendency depending on alteration

degrees. But the only Au ore (BLR-034) shows the highest polarization value of 8.7% and this may give some indication on the rock propety in this area.

Fig.34 Frequency Distribution of Polarization of Rocks

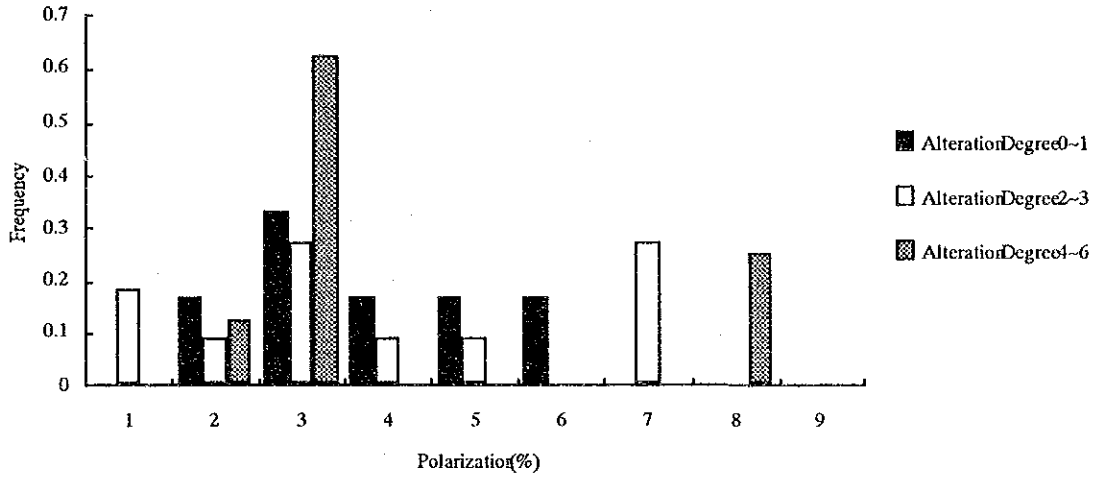

From the view point of chemical composition of fresh rocks, dacite shows high polarization of 6.4%, andesitic rocks show polarization between 2.3% and 5.0%, average being 3.93%, and basalt shows polarization of 3.8%. This cannot be regarded as a tendency of rock property of this area, but according to the result the more acidic a rock's composition becomes, the larger polarization it shows.

3-3 Geochemical Survey (Rock)

Rock geochemical survey was carried out in the Detiled Survey Area. Geochemical and geological surveys were conducted at the same time. Sampling points were selected to cover the whole area. Total number of taken samples is 104.

3-3-1 Pathfinder and Analytical Methods

Following 11 elements were selected for pathfinder elements:

Au,Ag,As,Sb,Hg,Cu,Pb,Zn,Mo,Fe,S

Analytical methods and detection limits are the same as those of stream sediment geochemical survey in Catanduanes island.

3-3-2 Analysis of Geochemical Data

(1) Statistic Processing

Analytical data are shown in Appendix-10. Common logarithm was used in the statistic processing. For the assay values under the lower detection limits, the half values of the lower detection limits were used for caluculation. For the values over the upper detection limits, the values of the upper limits were used for calculation (Zn:10,000 ppm). Hg was excluded from the processing as most of values analyzed were under the detection limits.

Basic statistic values are shown in Table 33.

Au shows wide range of assay values from 30,400 ppb to less than 1 ppb. Pb and S also have wide range distribution of assay values. On the contrary, Mo has narrow distribution because most of values are under the detection limits.

Table 33 **Basic Statistic Values of the Elements (Rocks)**

Element	Unit	Maximun	Minimum	Average	Av.-log	Stand. Dev.
Au	ppb	30400	<1	545.606	0.931	1.145
Ag	ppm	7.8	<0.2	0.330	-0.826	0.365
As	ppm	110	<2	13.606	0.800	0.579
Cu	ppm	2610	2	97.548	1.540	0.467
Fe	%	12.8	0.15	3.088	0.452	0.198
Mo	ppm	25	<1	1.226	-0.177	0.323
Pb	ppm	8740	<2	190.144	0.987	0.980
S	%	6.05	<0.001	0.198	-1.805	0.982
Sb	ppm	4	<2	1.240	0.070	0.134
Zn	ppm	>10000	4	221.058	1.910	0.492

Scatter diagram and correlation coefficients of the data are shown in Fig.35 and Table 34 respectively.

Au has comparatively strong positive correlation with Pb and moderate to weak positive correlation with As, Ag and Cu. Ag has weak positive correlation with Au, Cu and S. As has moderate positive correlation with Au and weak positive correlation with Pb. Cu has moderate positive correlation with Pb, Zn, and weak correlation with Au and Ag. Fe has weak positive correration with Zn. Pb has relatively strong positive correlation with Au, and moderate to weak positive correlation with As, Cu and Zn. S has weak positive correlation with Ag. Zn has moderate to weak positive correlation with Cu, Pb and Fe.

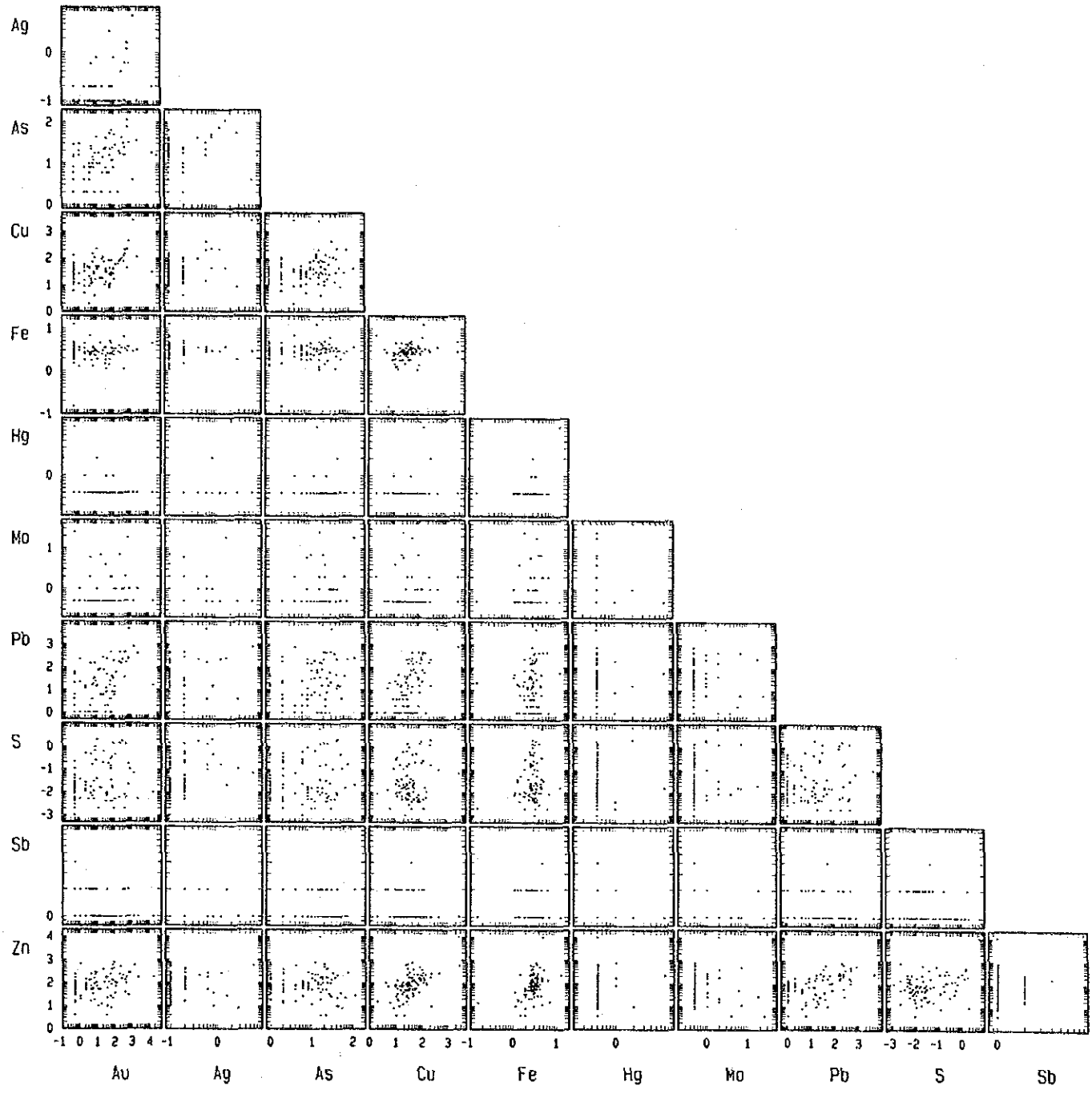

Fig.35 Scatter Diagram (rocks, Detailed Survey Area)

Table 34 **Correlation Coefficients brtween Elements (Rocks)**

	Au	Ag	As	Cu	Fe	Mo	Pb	S	Sb	Zn
Au	1.000									
Ag	0.454	1.000								
As	0.521	0.268	1.000							
Cu	0.487	0.490	0.208	1.000						
Fe	0.087	0.095	0.111	0.298	1.000					
Mo	0.250	0.197	0.351	0.057	0.081	1.000				
Pb	0.695	0.371	0.469	0.581	0.073	0.224	1.000			
S	0.283	0.469	0.055	0.246	0.098	0.091	0.222	1.000		
Sb	-0.136	0.048	-0.090	-0.115	0.030	-0.056	-0.046	-0.079	1.000	
Zn	0.390	0.244	-0.022	0.576	0.409	-0.189	0.489	0.213	-0.023	1.000

(2) Classification of Anomalous Values

Frequency distribution and cumulative frequency distribution are shown in Fig.36. Mean value and standard deviation together with frequency distribution and cumulative frequency distribution curves were used to set threshold values. For elements Au, Ag, As, Cu, Pb, Mo and S, two steps of classifications (anomaly values)are set to distinguish high anomalies. This classifications are shown in Table 35.

Table 35 **Classification of Geochemical Anomalies (Rocks)**

Au	M+σ (118.948ppb)	M+2 σ(1659.042ppb)
Ag	M+σ (0.346ppm)	M+2.5 σ(1.222ppm)
As	M+σ (23.929ppm)	M+1.5 σ(46.616ppm)
Cu	M+σ (101.607ppm)	M+2 σ(297.524ppm)
Fe	M+σ (4.470%)	
Mo	M+σ (1.401ppm)	M+2.5 σ(4.273ppm)
Pb	M+σ (92.689ppm)	M+2 σ(885.584ppm)
S	M+1.5 σ (0.467%)	M+2 σ(1.447%)
Sb	M+σ (1.596ppm)	
Zn	M+σ (261.417ppm)	

3-3-3 Distribution of Anomalous Areas

Distribution of geochemical anomalies are shown in Fig.37.

(Au) Relatively strong and wide anomalies of Au are distributed in the southern part of the Campo Mineral Occurrence. A small spot anomaly is in the northern part of the Occurrence. On the other hand, in the Gata Mineral Occurrence, the strong and relatively sizable anomalaly is located in the southern part, and there are spotted anomalies in the eastern part.

(Ag) In the Campo Mineral Occurrence, Ag anomaly extends from the southwest to the northeast of the area. There is also an anomaly of Ag in the eastern part of the Gata Mineral Occurrence.

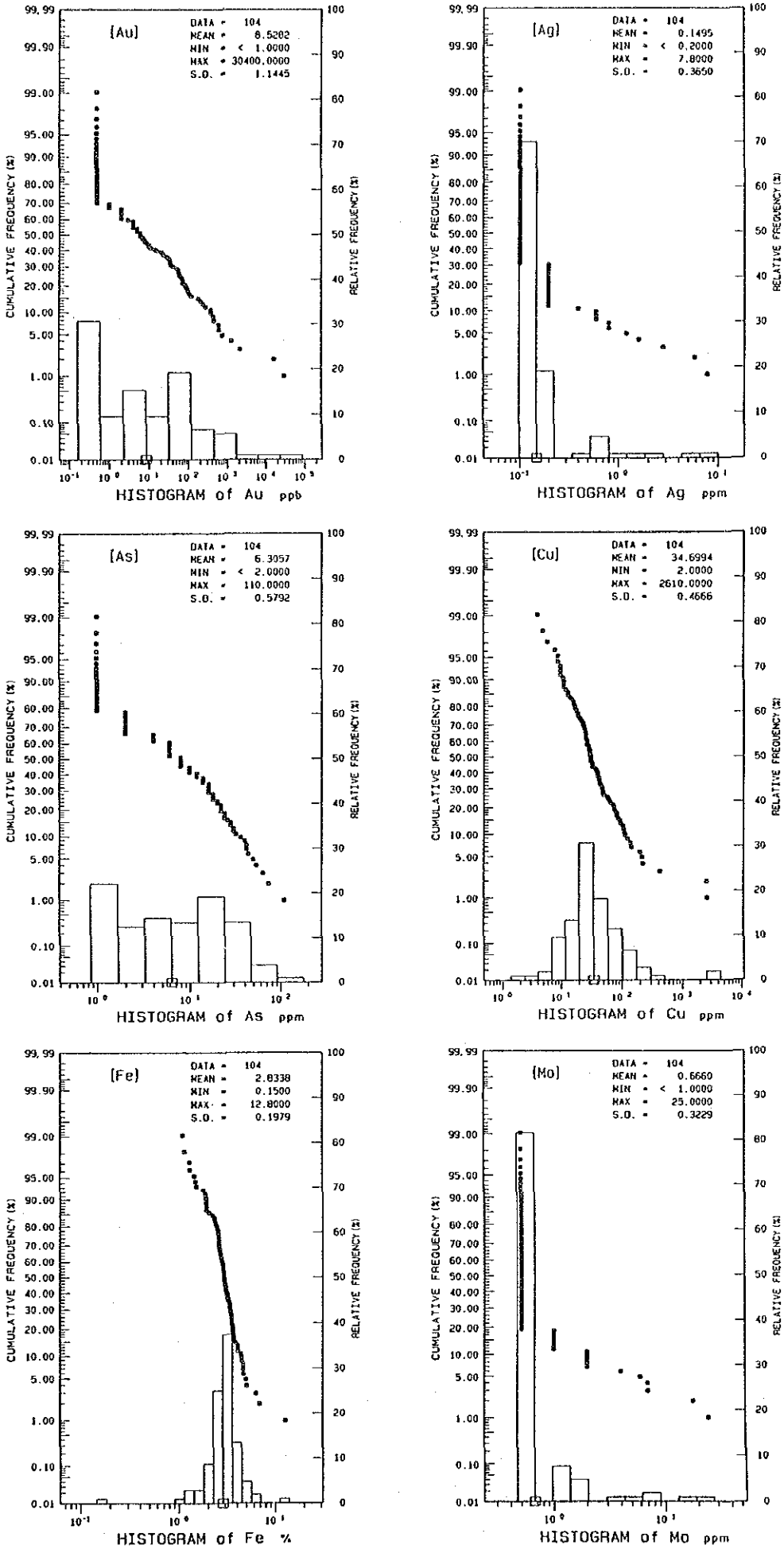

Fig.36 Frequency Distribution and Cumulative Frequency Distribution (rocks, Detailed Survey Area)(1)

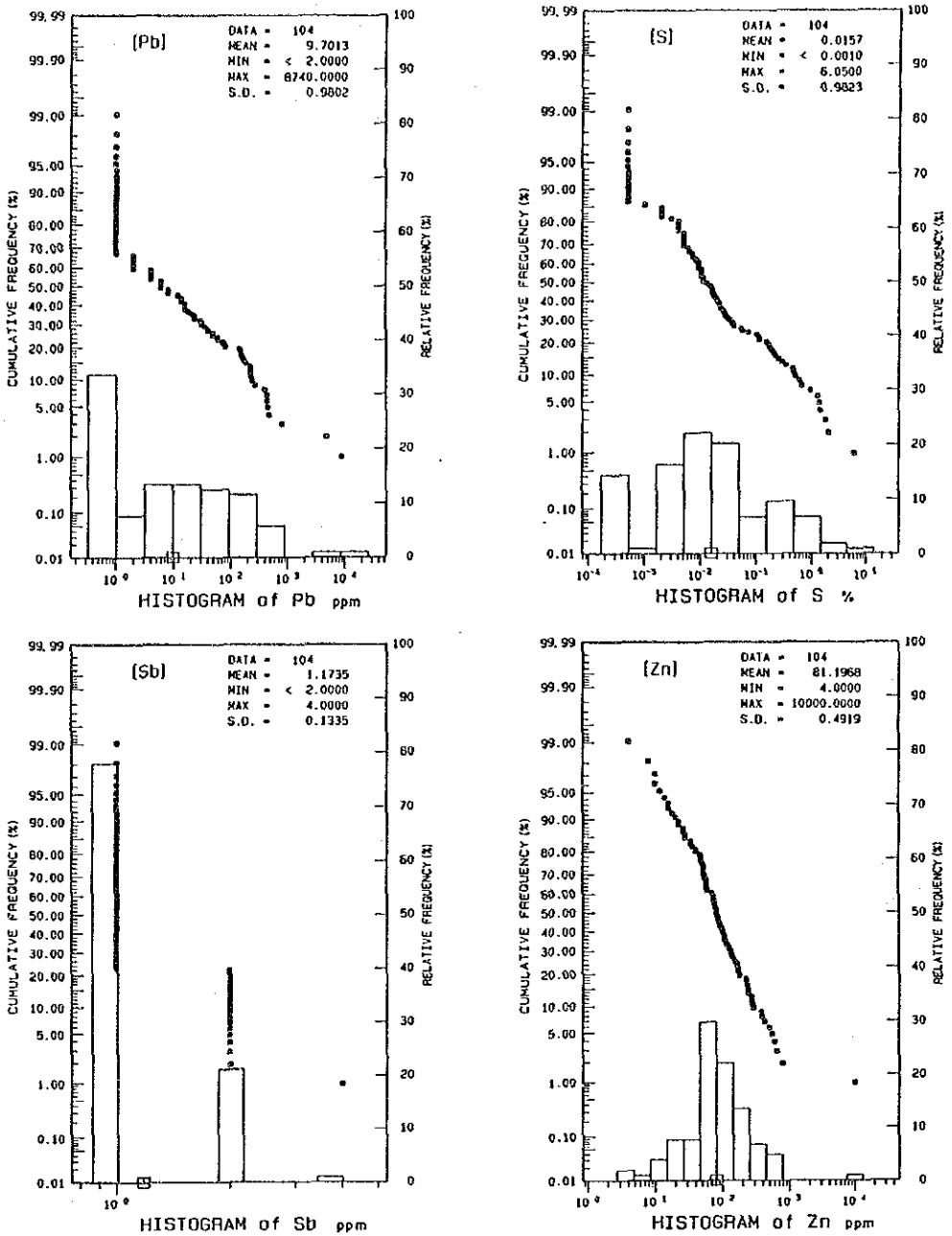

Fig.36 Frequency Distribution and Cumulative Frequency Distribution (rocks, Detailed Survey Area)(2)

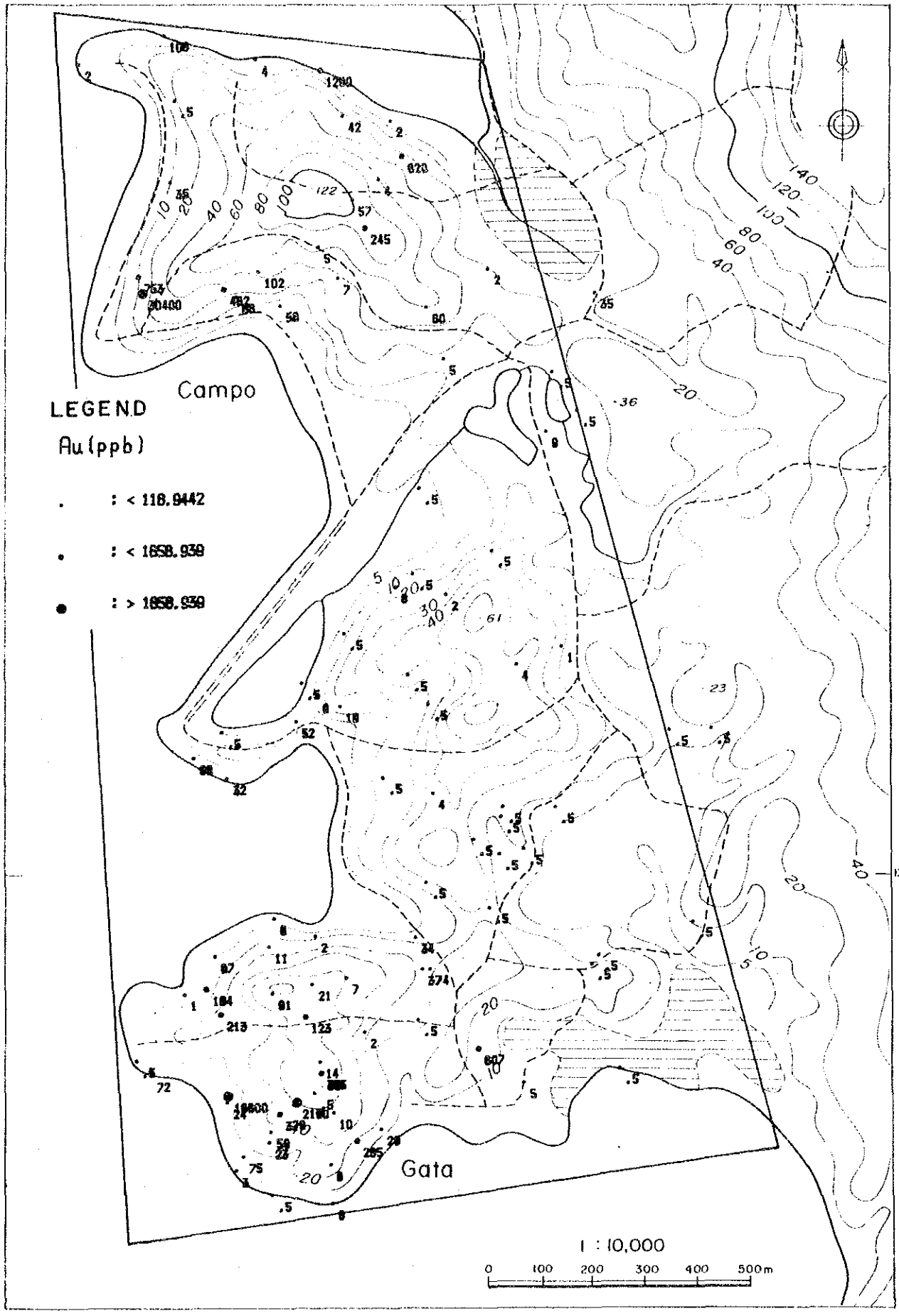

Fig.37 Distribution of Geochemical Anomalies (rocks, Detailed Survey Area)(1)

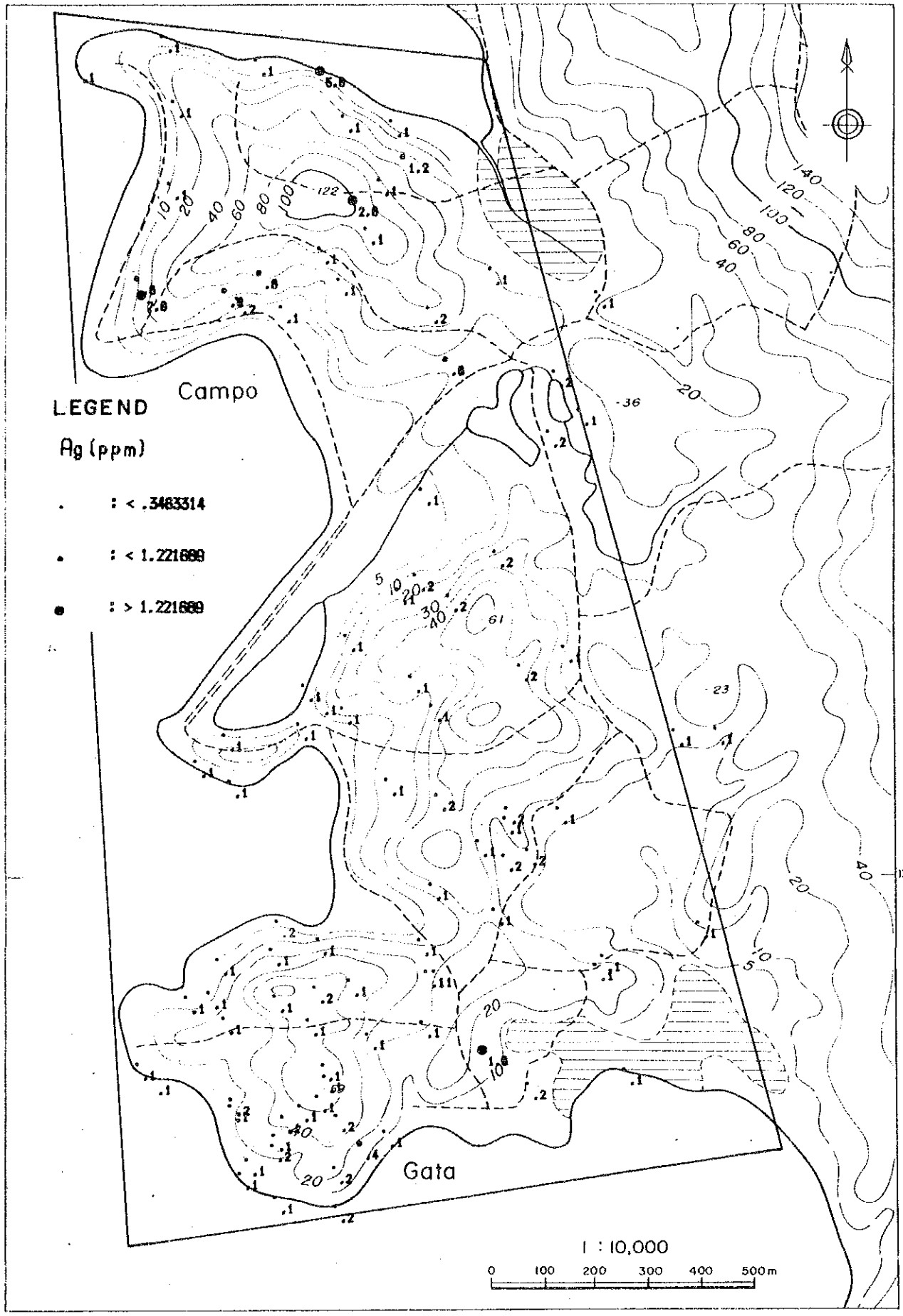

Fig.37 Distribution of Geochemical Anomalies (rocks, Detailed Survey Area)(2)

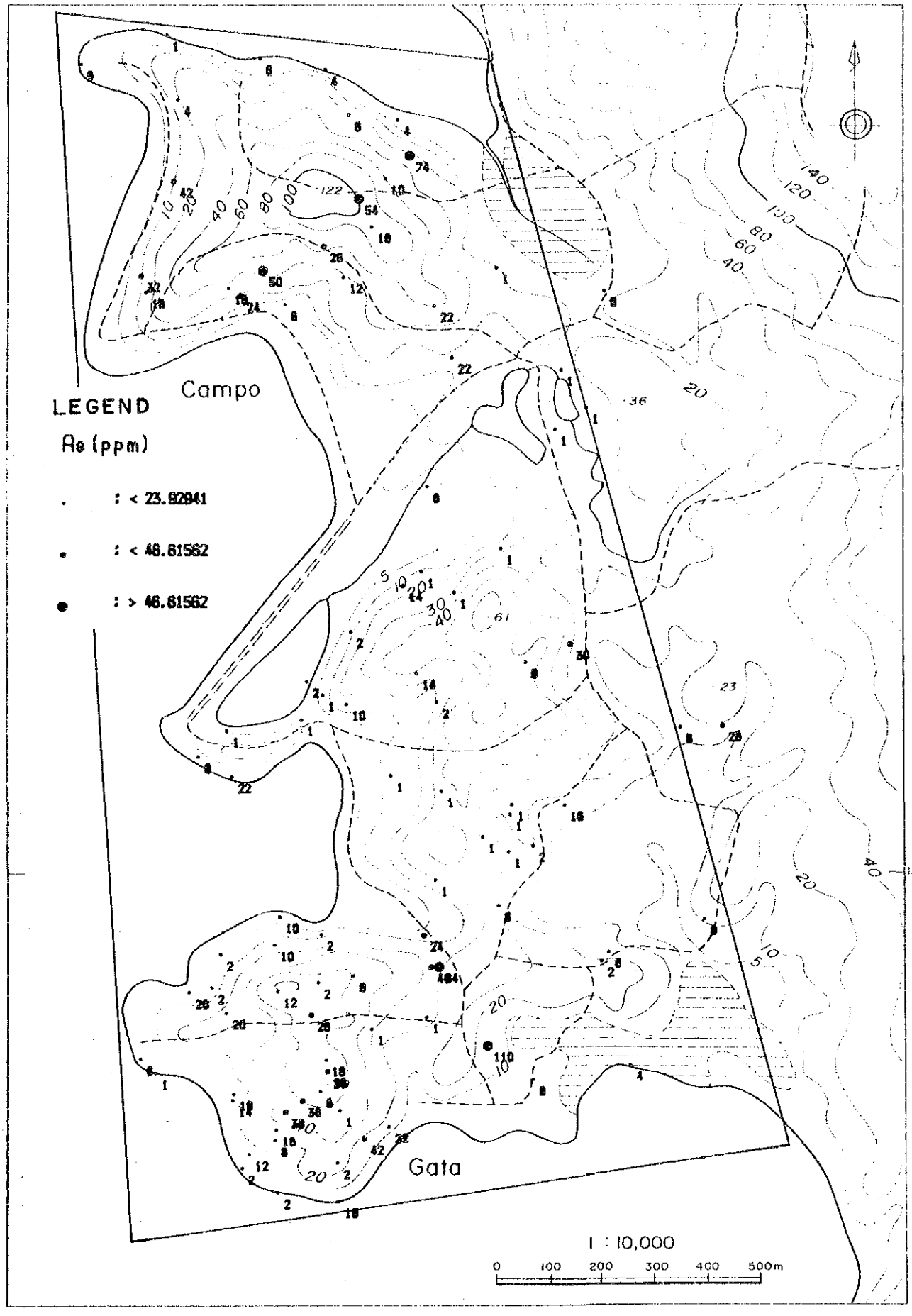

Fig.37 Distribution of Geochemical Anomalies (rocks, Detailed Survey Area)(3)

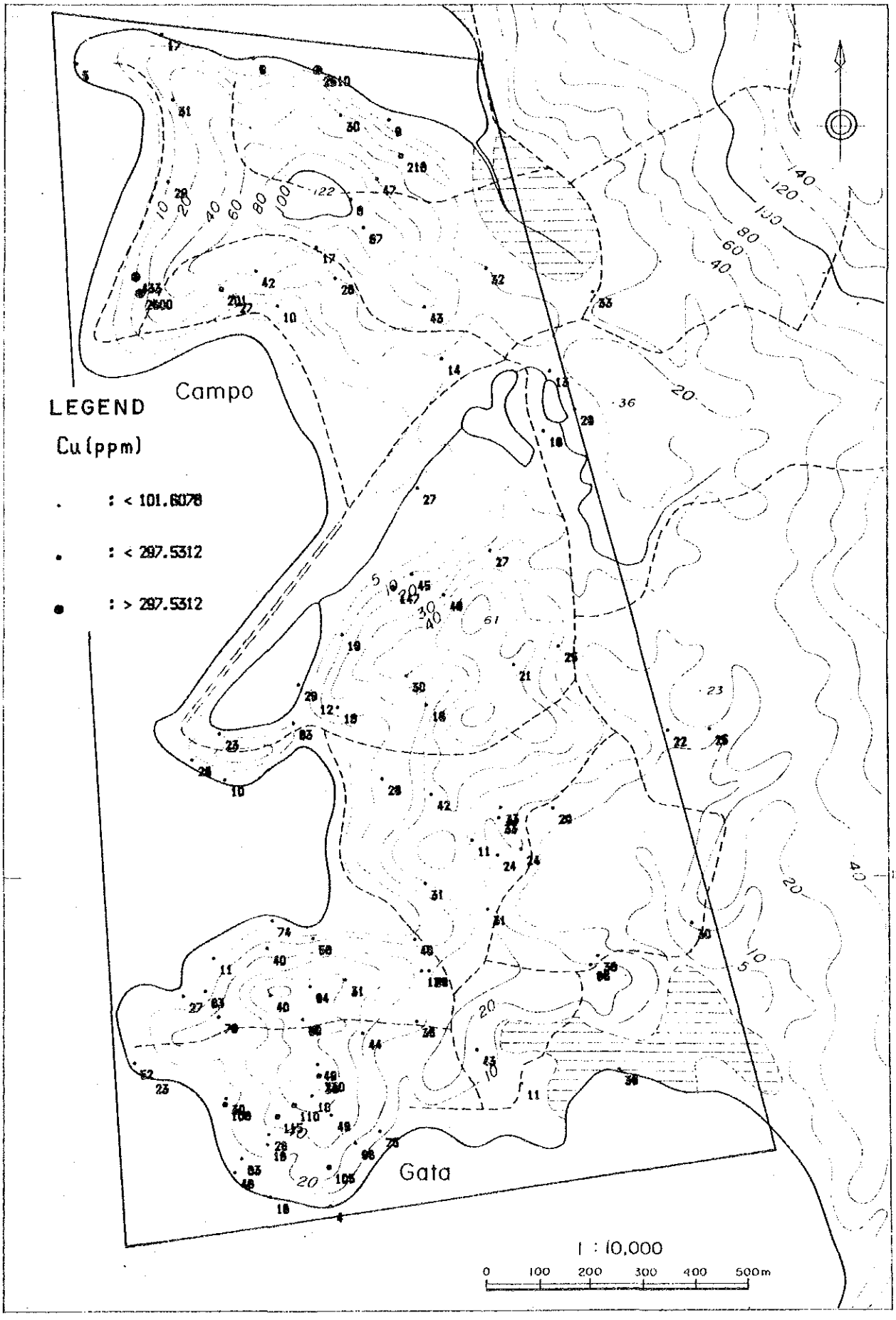

Fig.37 Distribution of Geochemical Anomalies (rocks, Detailed Survey Area)(4)

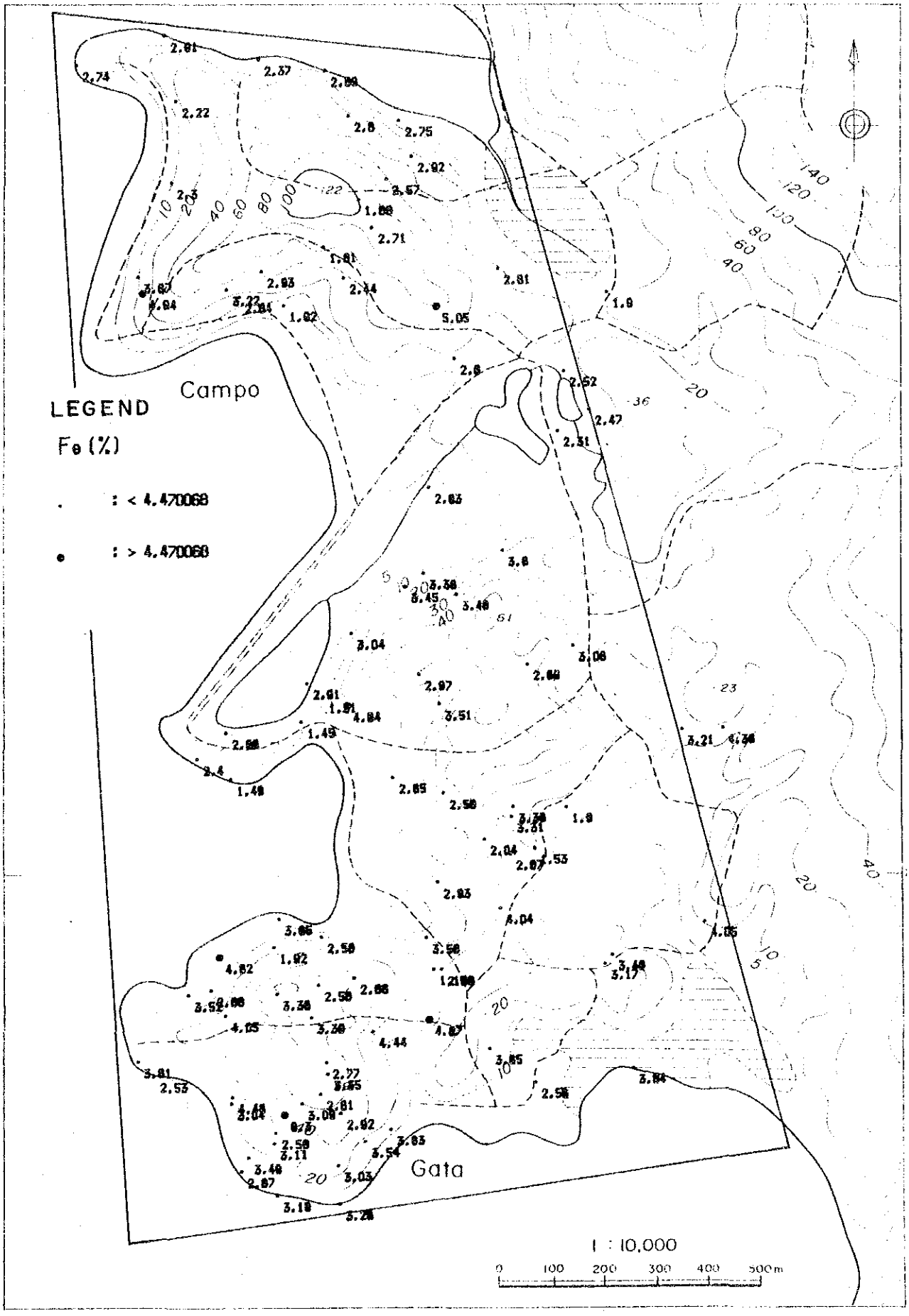

Fig.37 Distribution of Geochemical Anomalies (rocks, Detailed Survey Area)(5)

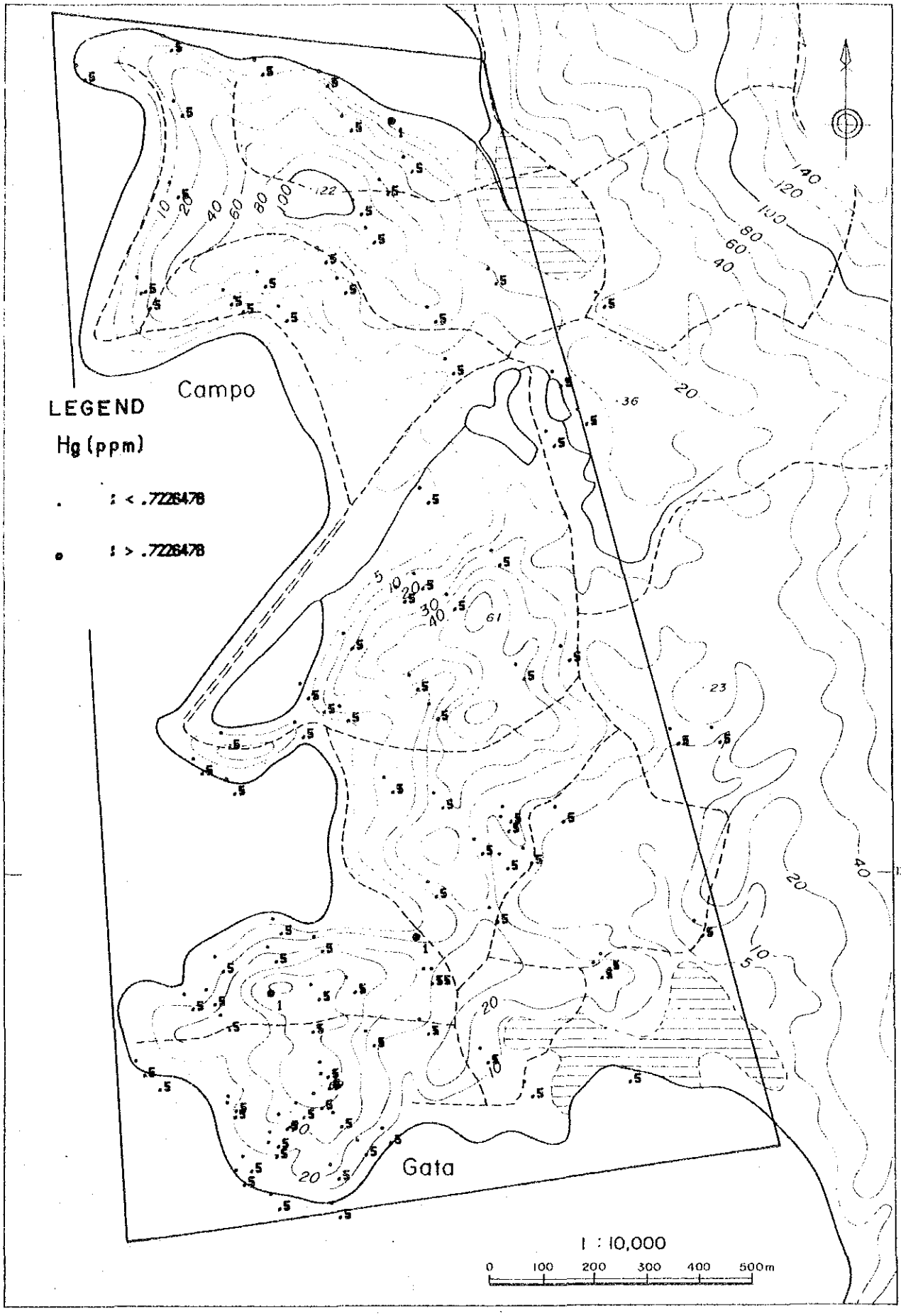

Fig.37 Distribution of Geochemical Anomalies (rocks, Detailed Survey Area)(6)

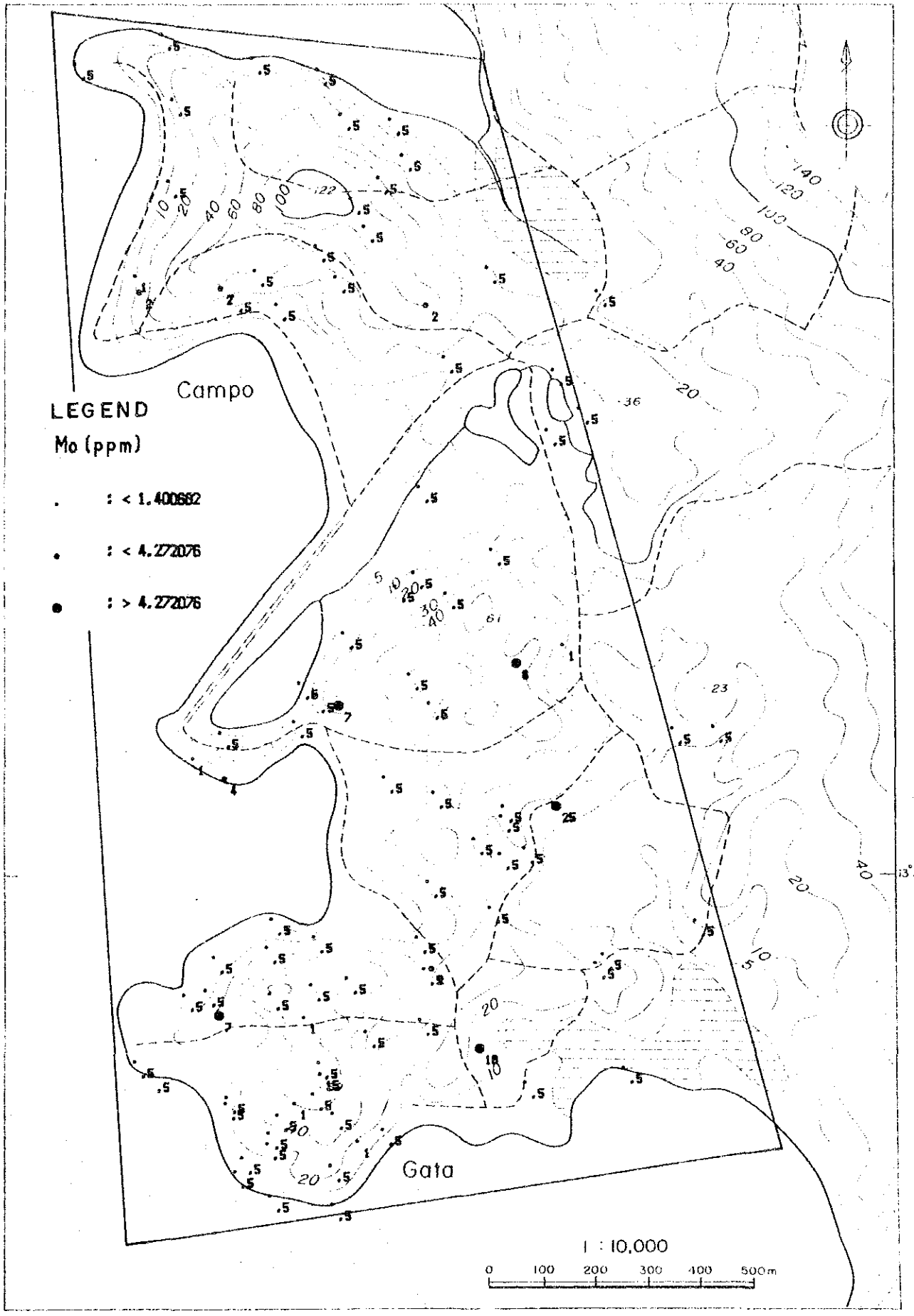

Fig.37 Distribution of Geochemical Anomalies (rocks, Detailed Survey Area)(7)

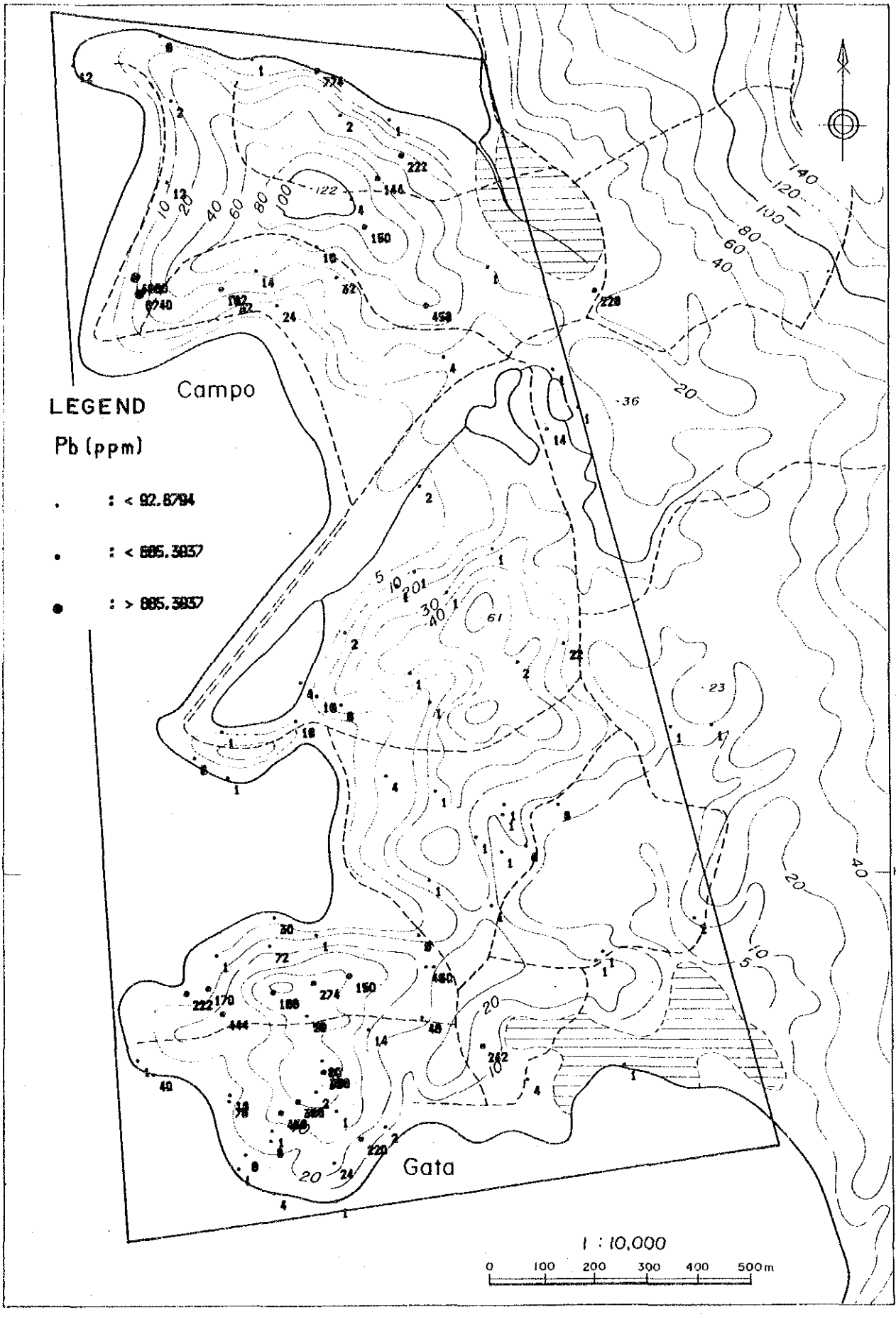

Fig.37 Distribution of Geochemical Anomalies (rocks, Detailed Survey Area)(8)

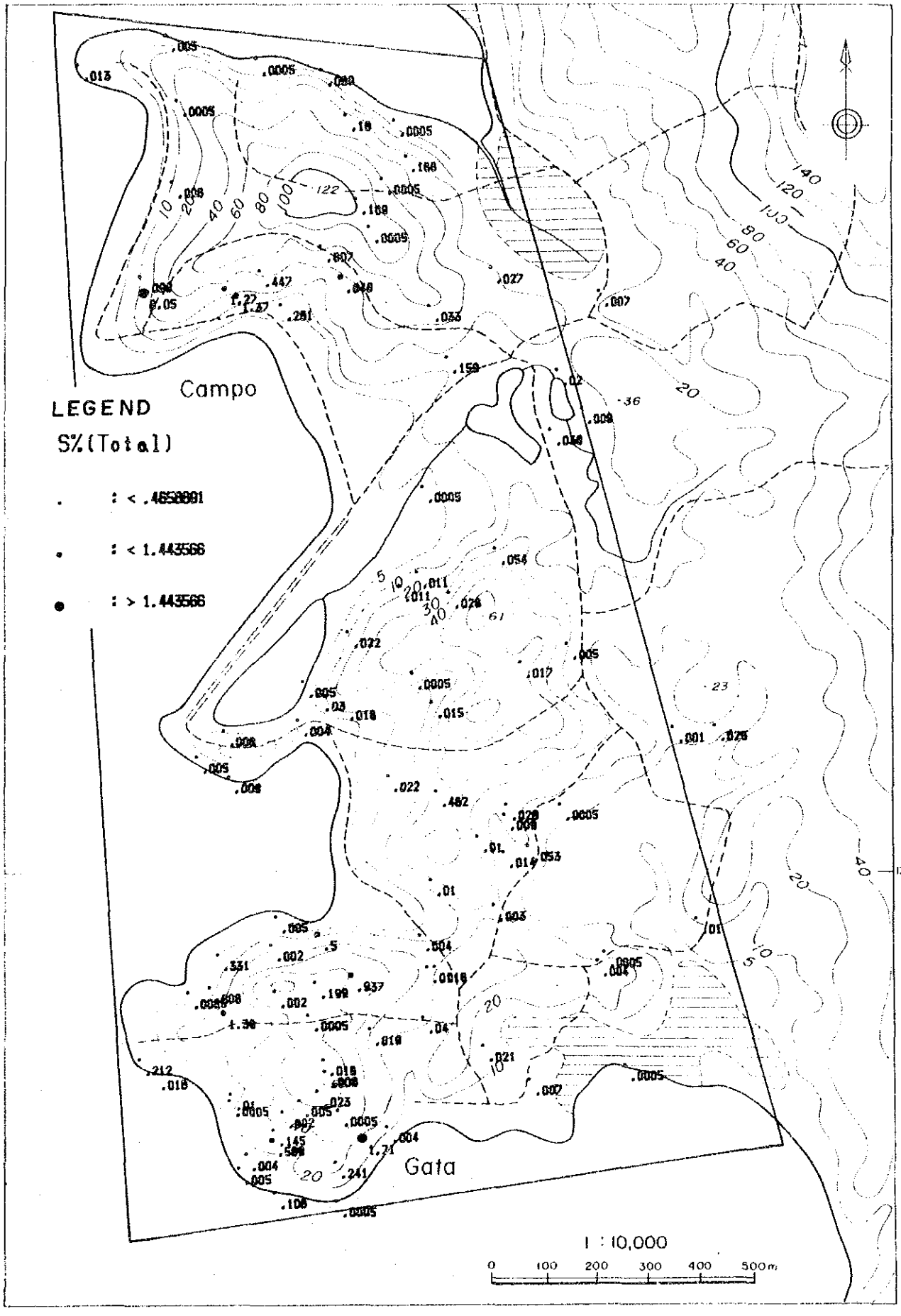

Fig.37 Distribution of Geochemical Anomalies (rocks, Detailed Survey Area)(9)

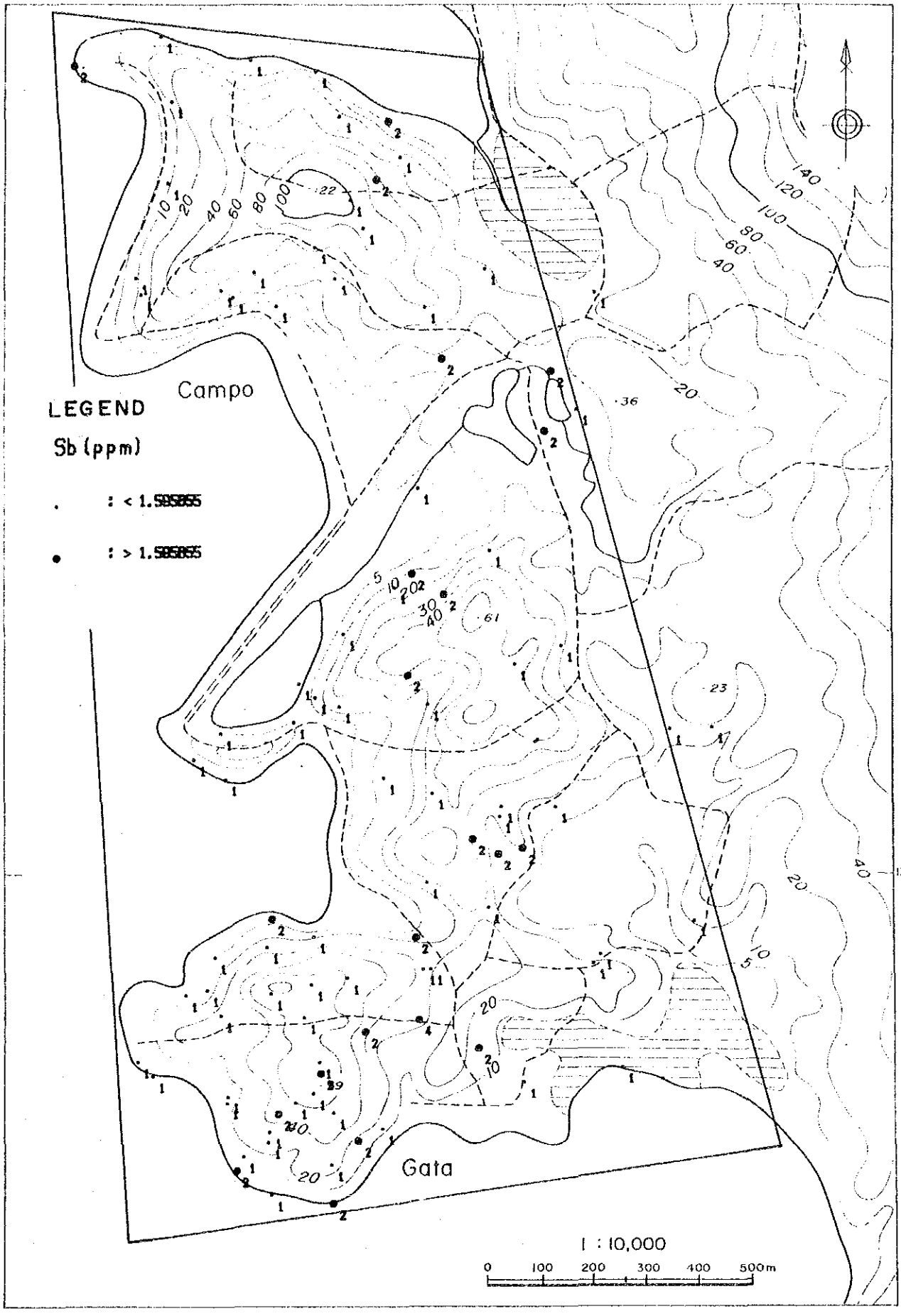

Fig.37 Distribution of Geochemical Anomalies (rocks, Detailed Survey Area)(10)

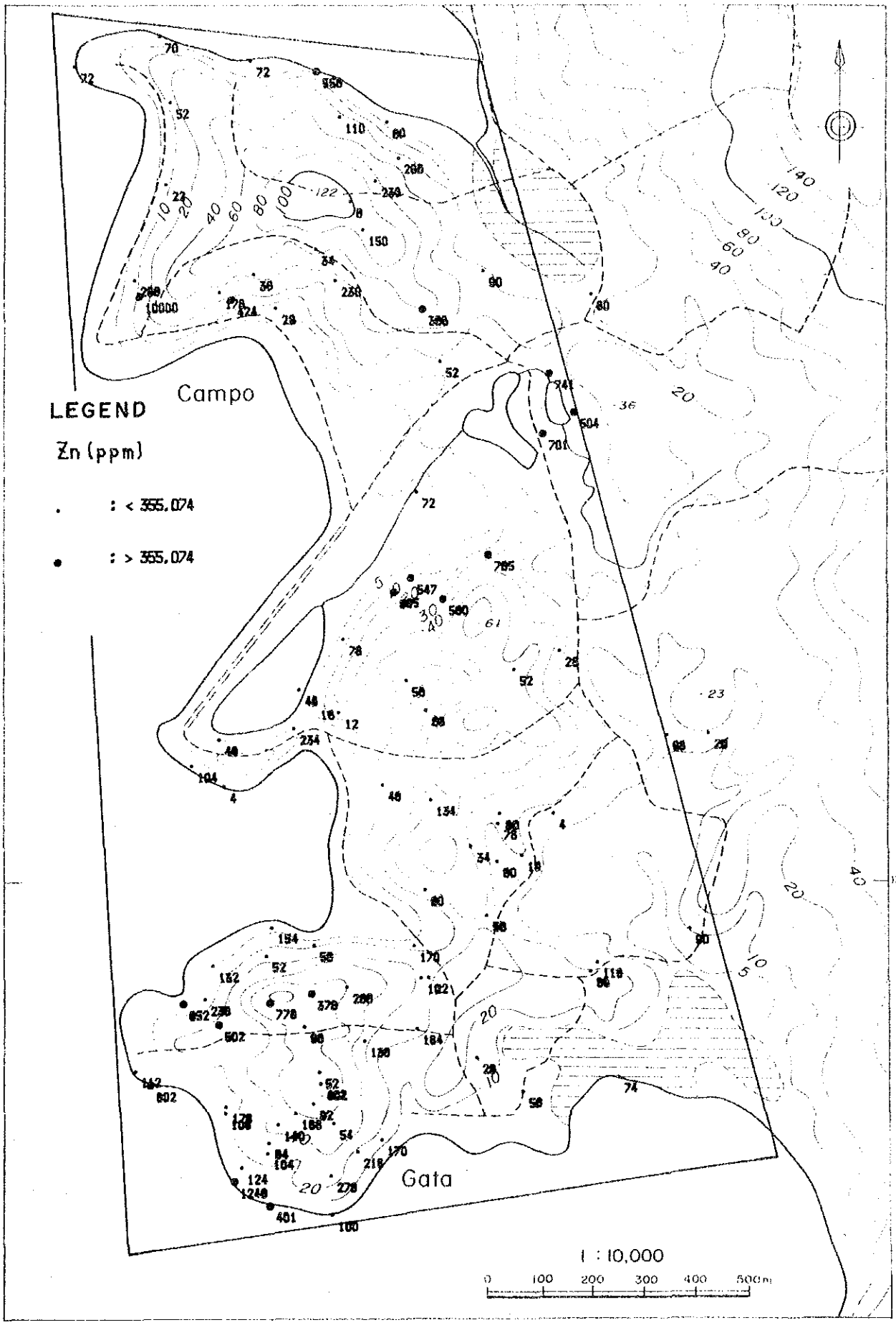

Fig.37 Distribution of Geochemical Anomalies (rocks, Detailed Survey Area)(11)

(As) A strong anomaly of As exists in the area extending from the south to northeast of the Campo Mineral Occurrence and a moderate anomaly is distributed along the western part of the Campo Mineral Occurrence. There are strong anomaly in the eastern part and weak anomaly in the central to western part of the Gata Mineral Occurrence.

(Cu) Strong anomaly of Cu are distributed in the southwestern part and northern part of the Campo Mineral Occurrence. Moderato to weak anomalies exist in the southern and eastern part of the Gata Mineral Occurrence. There is a weak spot anomaly between both Occurrences.

(Fe) There are spotted anomalies in the southwestern and southeastern ends of the Campo Mineral Occurrence and sporadic anomalies in the periphery of the Gata Mineral Occurrence.

(Mo) Spotted anomalies are scattered in the area from the Campo Mineral Occurrence to the Gata Mineral Occurrence.

(Pb) There are Pb anomalies in the southern part, eastern part and northern part of the Campo Mineral Occurrence. There are anomalies in the central part and eastern part of the Gata Mineral Occurrence.

(S) Anomalies of S are distributed in the southen part of the Campo Mineral Occurrence and there are some anomalies in the Gata Mineral Occurrence. There is a spot anomaly between the two Occurrences.

(Sb) There is wide anomaly zone in the southeastern half and a spot anomaly in the northern part of the Gata Mineral Occurrence. There are spot anomalies in the northern part and at the northwestern end of the Campo Mineral Occurrence. There are three small anomaly zones between the two Occurrence.

(Zn) Anomalies of Zn are distributed in the southern part and a spot anomaly in the northern part of the Campo Mineral Occurrence. In the Gata Mineral Occurrence, anomalies are distributed in the northern, western, southern part. Besides, there are two anomaly zones around the water reservoirs.

3-3-4 Pricipal Component Analysis

Correlation matrix , shown in Table 34, was used for the Principal Component Analysis (hereafter abbreviate it as PCA). Hg was excluded from the analysis because most of the assay values are under the lower detection limits. Results of PCA and scores of PCA are shown in Table 36 and Fig. 38 respectively.

Table 36 **Results of PCA (Rocks)**

Eigen value				Factor Loading					
P.C.	E.V.	Con.	CumCon		Z-01	Z-02	Z-03	Z-04	Z-05
Z-01	3.446	34.455	34.455	Au	0.819	0.206	-0.094	-0.106	-0.194
Z-02	1.554	15.537	49.992	Pb	0.819	0.086	-0.183	-0.043	-0.323
Z-03	1.087	10.867	60.859	Cu	0.774	-0.300	-0.065	-0.063	-0.022
Z-04	1.031	10.310	71.169	Ag	0.666	0.063	0.530	0.096	0.006
Z-05	0.946	9.461	80.630	Mo	0.289	0.667	-0.021	0.285	0.374
Z-06	0.589	5.887	86.516	As	0.535	0.571	-0.291	0.135	-0.037
Z-07	0.544	5.443	91.959	Zn	0.595	-0.667	-0.188	-0.030	-0.066
Z-08	0.344	3.437	95.395	S	0.464	-0.073	0.700	-0.148	0.281
Z-09	0.259	2.589	97.984	Sb	-0.127	-0.138	0.245	0.828	-0.449
Z-10	0.202	2.016	100.000	Fe	0.326	-0.412	-0.298	0.444	0.615

Abbreviations are as the same as Table 28.

Au, Ag, As, Cu and Pb showed strong positive correlation among themselves as shown in Table 32. The obvious results were obtained from the principal component analysis. Eigenvalue and contribution ratio of the first principal component are as large as 3.45 and 34.5% respectively, and the component has about 30% of the explanatory component of the variance of the analyzed values. Eigenvalues up to the fifth principal component are almost more than 1.0. Each principal component has following characteristic factors.

First principal component: This component has large factor loadings of Au, Ag, Cu, Pb, Zn, As, and (S) and it implies the mineralization. The high score zones are distributed in the Campo Mineral Occurrence and Gata Mineral Occurrence. This is harmonious with the fact that the mineral deoposits of two Occurrences are Au and Ag bearing quartz veins with chalcopyrite and galena and sphalerite.

Second principal component: This component is has large factor loadings of Mo, As, -Zn and (-Fe). Positive strong to weak scores are distributed in the central part or eastern part of the two Occurrences. Besides, high scores are scattered in the area between the two Occurences.

Third principal component: This component has large factor loading of S and Ag. Positive high score zones exist in the Campo Mineral Occurrence and within dacite dyke. Negative high scores are distributed widely in the central part of the Gata Mineral Occurrence and partly in the Campo Mineral Occurrence.

Fourth and fifth principal component: Thease components have large factor loadings of Sb and Fe. But Sb has not geological meaning because most of the assay values are under the detection limit. These two components have similar tendency. So, hereafter, explanation is based on the fifth component. Positive high to modererate scores are distributed in the western part of the Gata Mineral Occurrence and the central part of the surveyed area. Negative high to

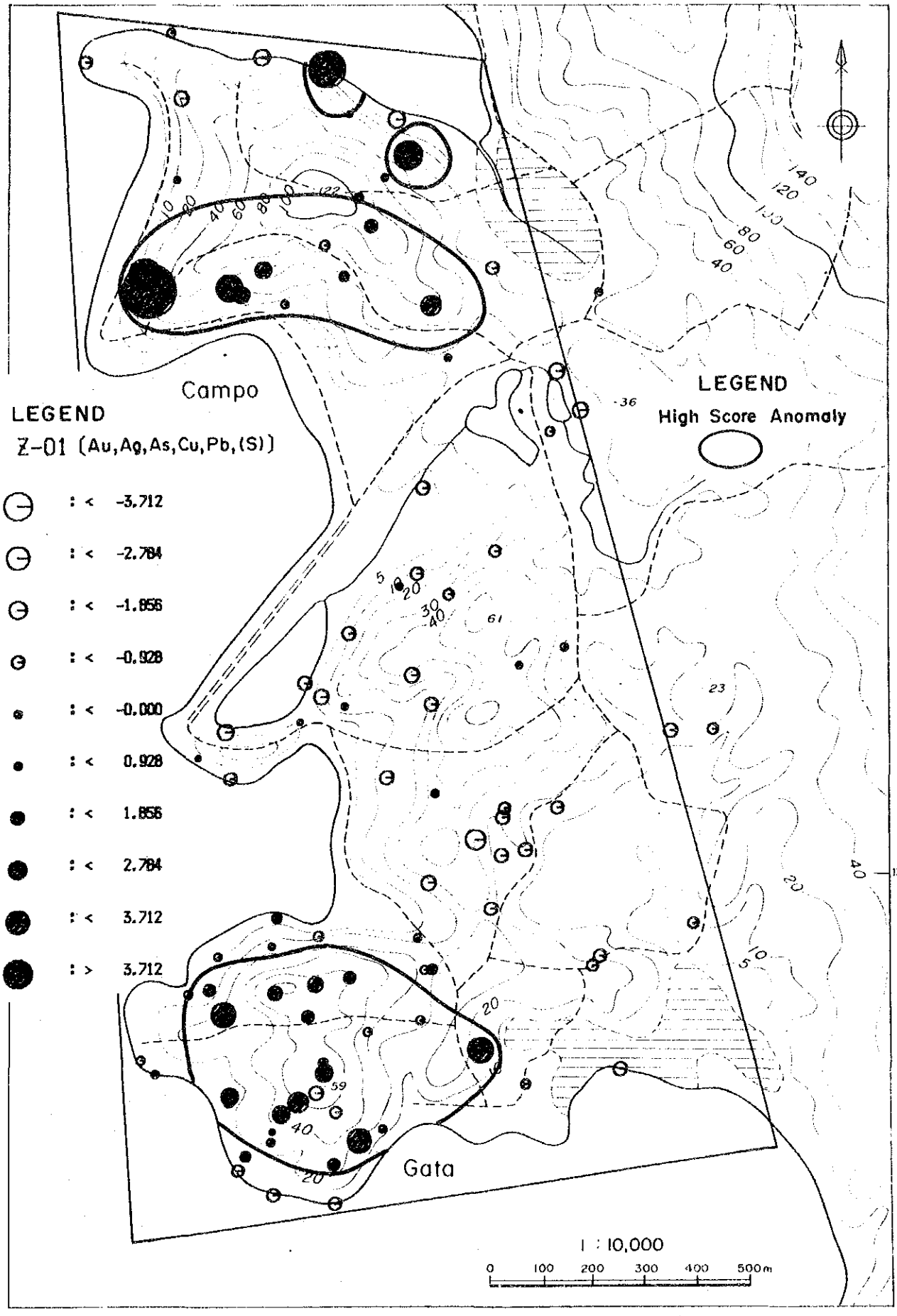

Fig.38 Distribution of PCA Scores (rocks, Detailed Survey Area)(1)

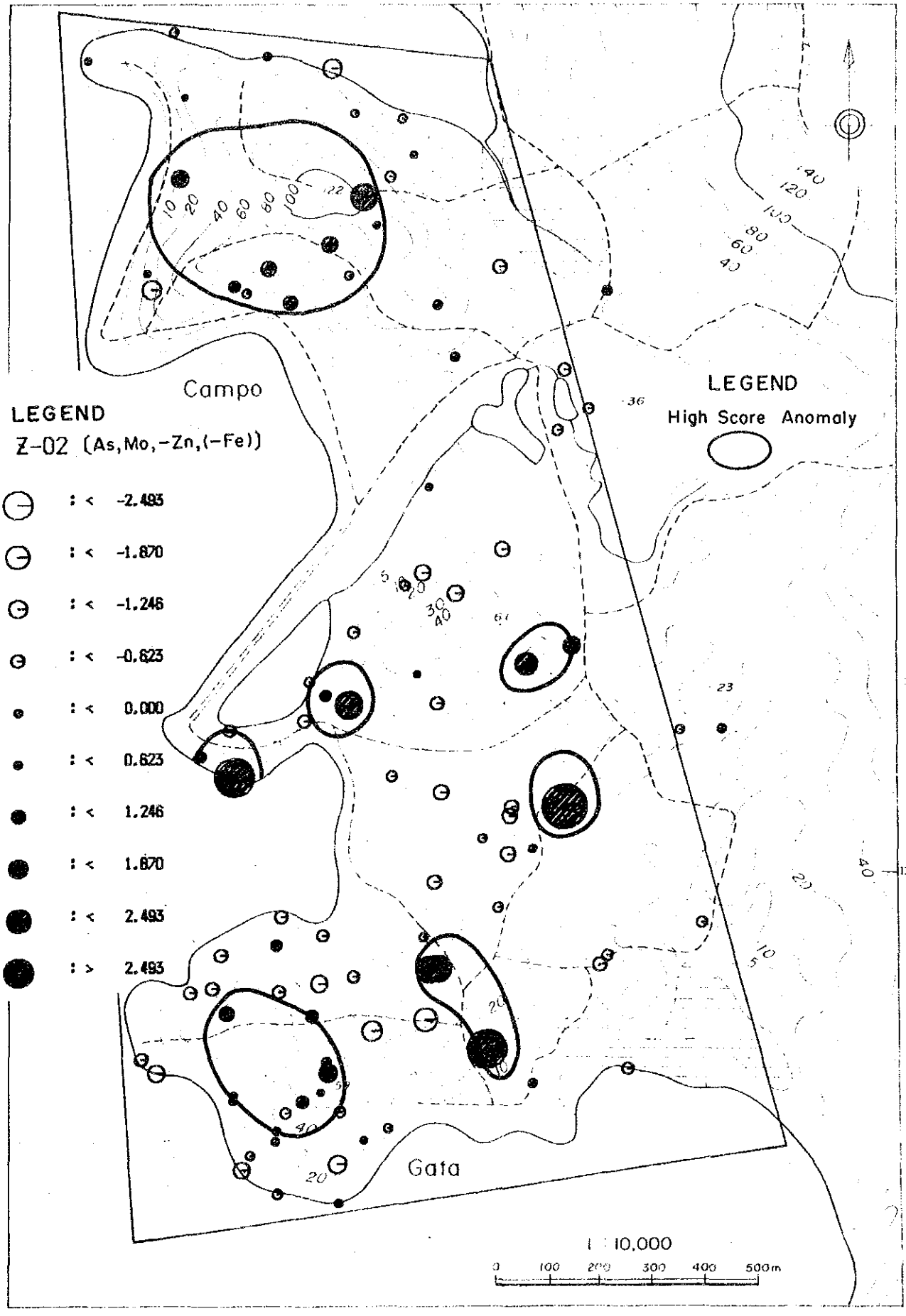

Fig.38 Distribution of PCA Scores (rocks, Detailed Survey Area)(2)

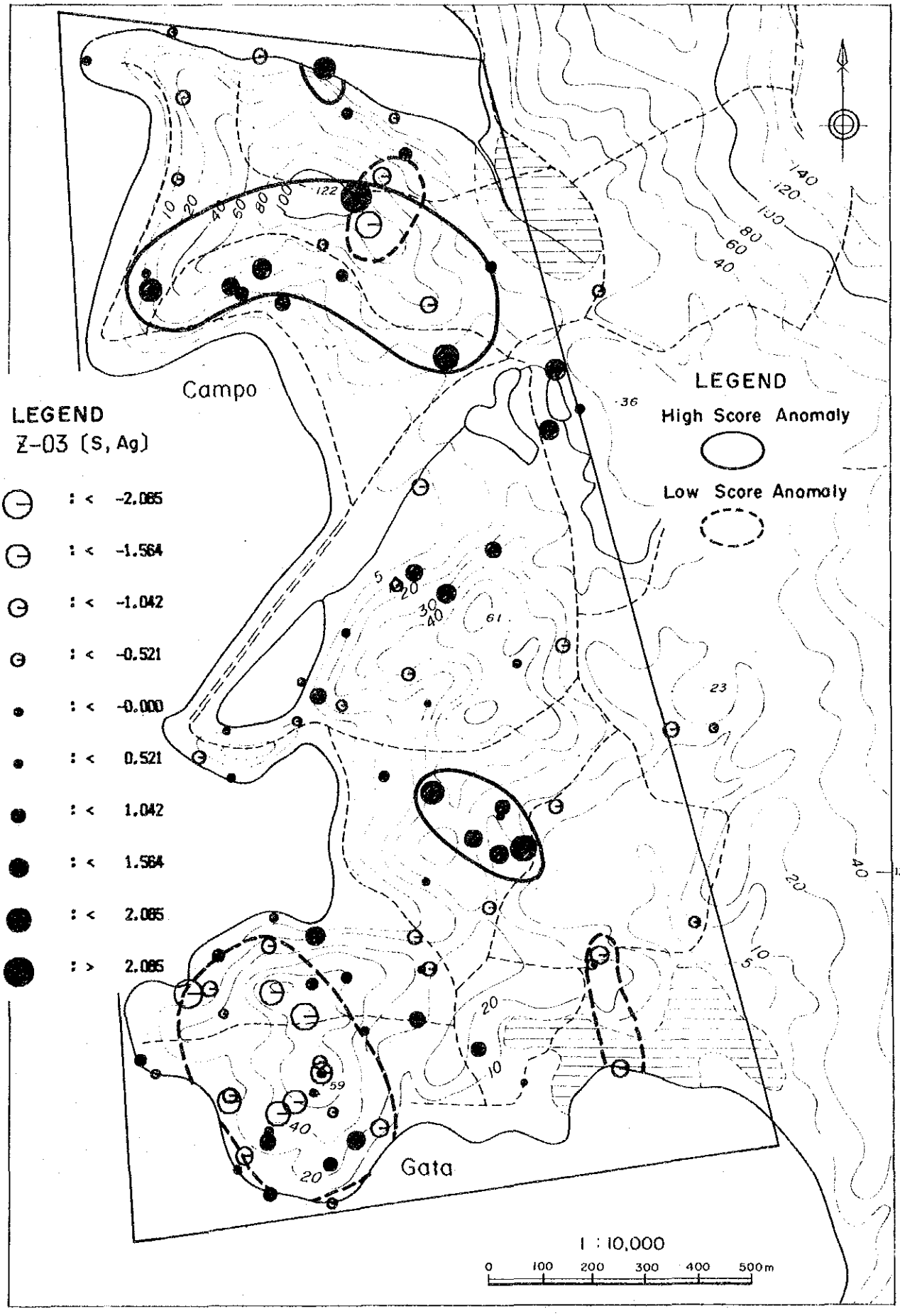

Fig.38 Distribution of PCA Scores (rocks, Detailed Survey Area)(3)

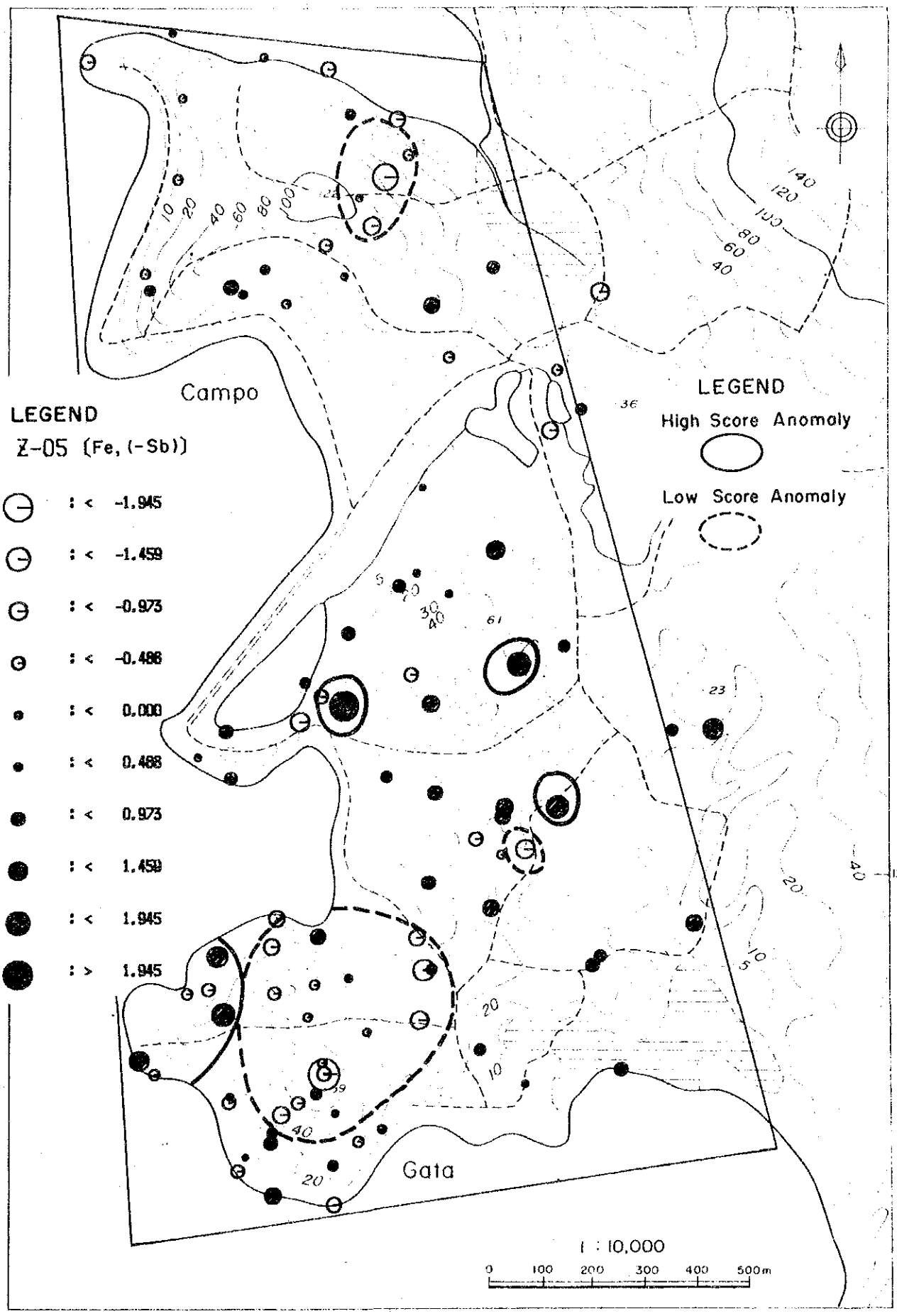

Fig.38 Distribution of PCA Scores (rocks, Detailed Survey Area)(4)